Contemporary Mathematics
http://ojs.wiserpub.com/index.php/CM/

UNIVERSAL WISER PUBLISHER

Research Article

The New Explanation of Lomax Distribution: Its Properties, Inference, and Applications to Real-Life Data

Hassan M. Aljohani

Department of Mathematics and Statistics, College of Science, Taif University, P.O. Box 11099, Taif 21944, Saudi Arabia
E-mail: hmjohani@tu.edu.sa

Received: 24 September 2024; **Revised:** 18 November 2024; **Accepted:** 7 January 2025

Abstract: This paper introduces an extended form of the Lomax model known as the new extended heavy-tailed Lomax (NEHTLx) distribution. The NEHTLx distribution features a failure rate that can exhibit various shapes, including unimodal, bathtub, reversed-J, and decreasing patterns. This versatility means that the failure rate function can have multiple peaks, making it potentially more suitable for fitting a wide range of data. The probability density function of the NEHTLx can be expressed as a combination of Lomax densities. The paper explores several mathematical properties of the NEHTLx distribution using various statistical tools. It also employs classical analytical methods to estimate the parameters of the NEHTLx model. To assess the performance of these estimation methods, comprehensive simulations are conducted for both small and large datasets. The ranking of these methods is analyzed using partial and overall ranks to evaluate their effectiveness. Additionally, the paper highlights the advantages of the NEHTLx distribution compared to traditional Lomax distributions through an analysis of two real-world datasets from applied domains, demonstrating its practical relevance and superior fitting capabilities.

***Keywords*:** Lomax distribution, maximum likelihood, wavelet methods, parameter estimation, medicine data, simulations

MSC: 60E05, 62F10

1. Introduction

In order to enhance the modelling of real-life survival data in several applicable domains, including environmental and biological sciences, finance, economics, and engineering, a number of continuous distributions have been presented and examined in the literature. The Lomax (Lx) distribution [1] is even known as the Pareto II distribution, and it only supplies a decreasing hazard rate (HR) as described in Chahkandi and Ganjali [2]. The Lx distribution plays a crucial role in advancing methodologies for signal and image estimation, particularly in handling complexities that arise from real-world data. Its ability to address heavy-tailed characteristics significantly contributes to the enhancement of both the accuracy and the reliability of estimation processes. Consequently, it has to provide a better fit to real-world data sets that often have bathtub-shaped or upside-down bathtub-shaped failure rates, which are common in biological and engineering dependability research. According to Balkema and de Hann [3], it is a limiting distribution of residual lifespan at a considerable age-see Johnson et al. [4] and Arnold [5] for additional details regarding the Lx distribution.

DOI: https://doi.org/10.37256/cm.6220255778

The extensions of the Lx distribution have found wide applications in many research areas. These include income and wealth disparity, medical and biological sciences, engineering, size of cities, actuarial science, and lifetime and reliability modeling. The impact of these extensions is seen in a variety of models, including the Marshall-Olkin Lx [6], exponentiated Lx [7], McDonald Lx, beta Lx, and Kumaraswamy-Lx (KwLx) [8], gamma Lx [9], Weibull Lx [10], odd exponentiated half-logistic Lx (OEHLLx) [11], extended odd Weibull Lomax (EOWLx) model [12], beta exponentiated Lx (BELx) [13], Fréchet Topp-Leone Lx (FTLLx) [14], power-Lx (PLx) [15], alpha-power power-Lx [16], Lambert-Lx [17], and new exponential-Lx [18] models, among others.

This paper presents the new extended heavy-tailed Lx (NEHTLx) distribution, which is an expansion of the Lx model. The new extended heavy-tailed-G (NEHT-G) family and the Lx model serve as the foundation for the construction of the NEHTLx distribution [19]. Some of its mathematical properties are proven to confirm a good explanation. A reversed J-shaped and right-skewed density function is provided by the NEHTLx model. Its HR function (HRF) can handle unimodal, bathtub, reversed-J-shaped, and decreasing shape. Compared to other Lx competing distributions, such as the KwLx, OEHLLx, EOWLx, BELx, FTLLx, PLx, and Lx distributions, the NEHTLx distribution regularly yields better fits.

This article also explores several methodologies used to estimate the NEHTLx parameters. We thoroughly evaluate different estimators to identify the best estimation technique for the NEHTLx model. In this comparison, the mean square errors, absolute bias, and mean relative errors are used to evaluate the performance of the simulation experiments for both small and big samples. The best estimators for estimating the NEHTLx parameters are then found by ranking these measurements' outcomes using partial and overall ranks. The Lx distribution is explained twice, and several properties are defined for estimating wavelet coefficients.

Here is a summary of the remaining content in this article: NEHTLx distribution is introduced in Section 2. Section 3 presents the mathematical features of the suggested model. A variety of estimators for the NEHTLx unknown parameters are shown in Section 4. Section 5 discusses numerical simulations. The applicability of the NEHTLx model for real lifetime data sets is demonstrated in Section 6. Section 7 provides a summary of the research findings.

2. The NEHTLx distribution

In the NEHT-G family, suggested by Aljohani et al. [19], the Lx distribution is used as a baseline model to define the NEHTLx distribution in this section. The Lx distribution's cumulative distribution function (or CDF) has the following form

$$G(x;\ \delta,\ \lambda) = 1 - \left(1 + \frac{x}{\delta}\right)^{-\lambda},\ x > 0,\ (\lambda,\ \delta) > 0, \tag{1}$$

where λ is a shape parameter and δ is a scale parameter. The probability density function (PDF) corresponding to (1), is defined as

$$g(x;\ \delta,\ \lambda) = \frac{\lambda}{\delta}\left(1 + \frac{x}{\delta}\right)^{-\lambda-1}, \tag{2}$$

from (1) and (2)

$$1 - G(x;\ \delta,\ \lambda) = \frac{\delta}{\lambda}\left(1 + \frac{x}{\delta}\right)g(x;\ \delta,\ \lambda). \tag{3}$$

From (3), it is easy to extract that $\lim_{x\to\infty} G(x;\ \delta,\ \lambda)=1$ and $\lim_{x\to\infty} g(x;\ \delta,\ \lambda)=0$. Equation (3) shows the explanation the relation between $G(x;\ \delta,\ \lambda)$ and $g(x;\ \delta,\ \lambda)$. The corresponding HRF of (1) is

$$h(x;\ \delta,\ \lambda)=\frac{\lambda}{\delta}\left(1+\frac{x}{\delta}\right)^{-1}. \tag{4}$$

Let $G(x;\ \boldsymbol{\psi})$ be the baseline CDF with a parameter vector $\boldsymbol{\psi}$. Next, we define the CDF of the NEHT-G family as [19]

$$F(x;\ \beta,\ \alpha,\ \boldsymbol{\psi})=1-\left(\frac{1-G(x;\ \boldsymbol{\psi})}{1-\bar{\alpha}G(x;\ \boldsymbol{\psi})}\right)^{\beta}. \tag{5}$$

One way to express the NEHT-G density is as

$$f(x;\ \beta,\ \alpha,\ \boldsymbol{\psi})=\beta\alpha g(x;\ \boldsymbol{\psi})\frac{\left(1-G(x;\ \boldsymbol{\psi})\right)^{\beta-1}}{\left(1-\bar{\alpha}G(x;\ \boldsymbol{\psi})\right)^{\beta+1}},\quad \beta,\ \alpha>0,\quad x>0, \tag{6}$$

where β and α are two positive shape parameters, respectively and $\bar{\alpha}=(1-\alpha)$. Thus, by incorporating the CDF of the Lx (1) into Equation (5), the CDF of the NEHTLx distribution may be obtained as

$$F(x;\ \boldsymbol{\varphi})=1-\left(1+\alpha\left(\left(1+\frac{x}{\delta}\right)^{\lambda}-1\right)\right)^{-\beta},\quad x>0, \tag{7}$$

where $\boldsymbol{\varphi}=(\beta,\ \alpha,\ \delta,\ \lambda)^{\intercal}$. The PDF of the NEHTLx distribution can be written as

$$f(x;\ \boldsymbol{\varphi})=\frac{\beta\alpha\lambda}{\delta}\left(1+\frac{x}{\delta}\right)^{-\lambda\ \beta-1}\left(1-\bar{\alpha}\left(1-\left(1+\frac{x}{\delta}\right)^{-\lambda}\right)\right)^{-\beta-1},\quad x>0, \tag{8}$$

where for all $x>0$ and the positive quantities $\beta,\lambda,$ and α are the shape parameters and δ is the scale parameter.

Remark 1

• Setting $\beta=1$, $\alpha=1$, $\lambda=1$ and $\delta=1$ in (8), the results is

$$f(x)=\left(1+x\right)^{-2}=1-2x+3x^2-4x^3+\cdots=\sum_{n=1}^{\infty}(-1)^{n-1}nx^{n-1}, \tag{9}$$

hence the sum of (9) is converge to 1.

The HRF of the NEHTLx model is derived as

$$h(x;\,\boldsymbol{\varphi}) = \frac{\beta\alpha\lambda\left(1+\dfrac{x}{\delta}\right)^{-\lambda\ \beta-1}\left(1-\bar{\alpha}\left(1-\left(1+\dfrac{x}{\delta}\right)^{-\lambda}\right)\right)^{-\beta-1}}{\delta\ \left(1+\alpha\left(\left(1+\dfrac{x}{\delta}\right)^{\lambda}-1\right)\right)^{-\beta}}. \tag{10}$$

Figure 1a displays some shapes of the NEHTLx PDF for different values of its parameters as $\lambda \to 0$ the shape reaches zero quickly. The plots show that the NEHTLx density can be right-skewed, reversed-J shaped, or concave down. Figure 1b displays the CDF as $\lambda >> 1$ the shape reaches one quickly. Figure 1c shows the survival function (SF) as $\lambda \to 0$ the shape reach zero quickly. Figure 1c shows some shapes of the HRF of the NEHTLx model for some selected values of β, α, δ, and λ. The plots illustrate that the NEHTLx HRF exhibits bathtub, unimodal, reversed-J shaped, and decreasing hazard rates.

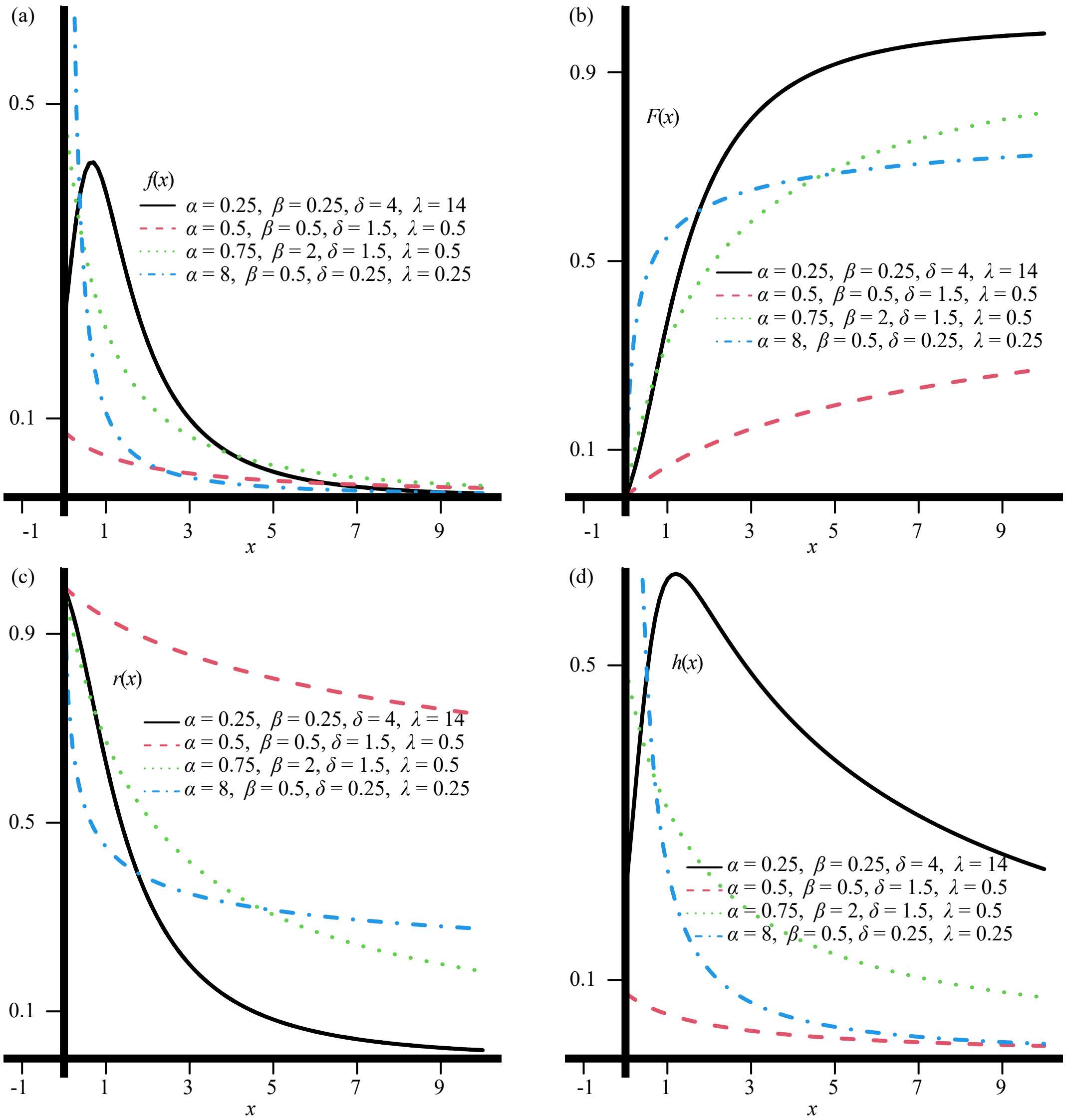

Figure 1. Plots of the PDF, CDF, SF and HRF of the NEHTLx distribution for different parametric values

3. Some properties

In this section, various mathematical quantities of the NEHTLx are presented.

3.1 *Linear representation*

Hence, two power series can be used to derive a linear mixture of the NEHTLx density

$$\left(1+\omega D\right)^{-\tau}=\sum_{j=0}^{\infty}\binom{-\tau}{j}\omega^{j}D^{j}, \tag{11}$$

and

$$\left(1-D\right)^{\tau}=\sum_{k=0}^{\infty}\binom{\tau}{k}(-1)^{k}D^{k}, \quad -1<D<1. \tag{12}$$

Applying the power series (11) to the expression $A=\left[1+\left(\alpha-1\right)\left(1-\left(1+\frac{x}{\delta}\right)^{-\lambda}\right)\right]^{-\beta-1}$, we get

$$A=\sum_{j=0}^{\infty}\binom{-\beta-1}{j}\left(\alpha-1\right)^{j}\left[1-\left(1+\frac{x}{\delta}\right)^{-\lambda}\right]^{j}. \tag{13}$$

Then, the PDF (8) reduces to

$$f(x;\,\boldsymbol{\varphi})=\frac{\beta\alpha\lambda}{\delta}\sum_{j=0}^{\infty}\binom{-\beta-1}{j}\left(\alpha-1\right)^{j}\left(1+\frac{x}{\delta}\right)^{-(\lambda\beta+1)}\left[1-\left(1+\frac{x}{\delta}\right)^{-\lambda}\right]^{j}. \tag{14}$$

The power series (12) may be applied to the final term of (14), which can be represented as $\left(1+\frac{x}{\delta}\right)^{-\lambda}<1$.

$$\left[1-\left(1+\frac{x}{\delta}\right)^{-\lambda}\right]^{j}=\sum_{k=0}^{\infty}\binom{j}{k}(-1)^{k}\left(1+\frac{x}{\delta}\right)^{-\lambda k}. \tag{15}$$

Hence, Equation (14) becomes

$$f(x;\,\boldsymbol{\varphi})=\frac{\beta\alpha}{\beta+k}\sum_{k,\,j=0}^{\infty}(-1)^{k}\binom{j}{k}\binom{-\beta-1}{j}(\alpha-1)^{j}\frac{\lambda(\beta+k)}{\delta}\left(1+\frac{x}{\delta}\right)^{-\lambda(\beta+k)+1}. \tag{16}$$

It is also can be expressed in a simple form as follows

$$f(x;\,\boldsymbol{\varphi})=\sum_{k,\,j=0}^{\infty}\xi_{k,\,j}\;g(x;\,\delta,\,\lambda(\beta+k)), \tag{17}$$

where $g(x;\ \delta,\ \lambda(\beta+k))$ is the PDF of the Lx distribution with parameters δ and $\lambda(\beta+k)$ and

$$\xi_{k,\ j} = \binom{j}{k}\binom{-\beta-1}{j}\frac{\beta\alpha(-1)^k(\alpha-1)^j}{(\beta+k)}. \tag{18}$$

Therefore, it is possible to express the NEHTLx PDF as a linear combination of Lx densities.

3.2 *Quantile function*

By solving the equation $F(Q(u)) = u$ in (7) for $Q(u)$ in terms of u, one may obtain the quantile function (QF) of the NEHTLx distribution, and this means

$$Q(u) = \left(\delta\left[\frac{(\bar{\alpha}-1)(1-u)^{\frac{1}{\beta}}}{\bar{\alpha}(1-u)^{\frac{1}{\beta}}-1}\right]^{-\frac{1}{\lambda}} - \delta\right), \tag{19}$$

where $0 < u < 1$. Setting $u = 0.25,\ 0.50$ and 0.75 in (19) yields the first quartile, median, and third quartile, respectively. The relationships between the parameters β, α, δ, and λ can be examined using the QF (19). Both the Moors' kurtosis (MK) [20] and Galtonś skewness (GS) [21]-also referred to as Bowley skewness-depend on the QF. The GS and MK are provided, respectively, by

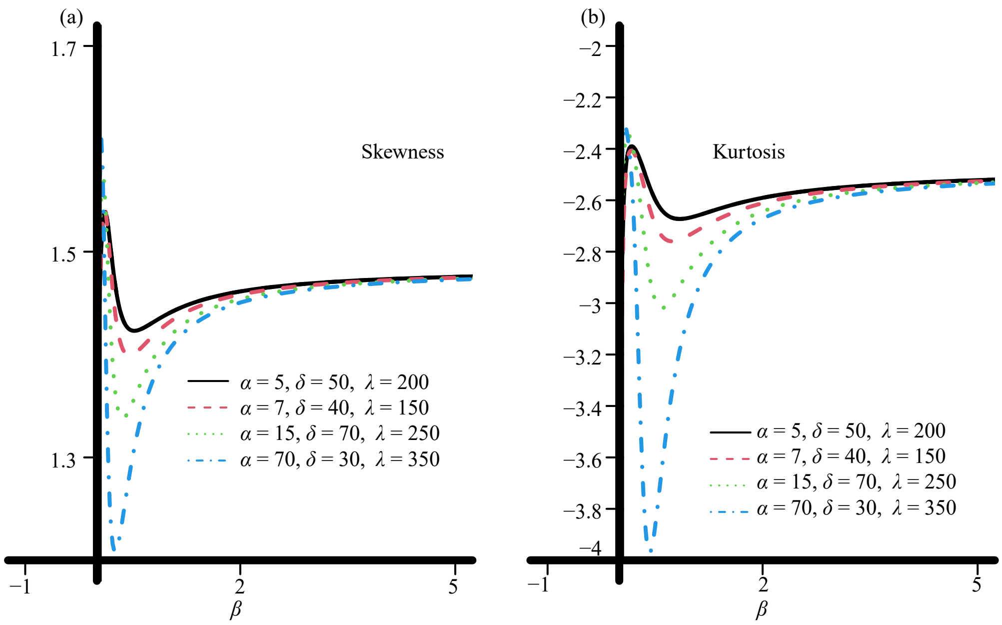

Figure 2. Plots of the GS and MK measures of the NEHTLx distribution for some parametric values

$$GS = \frac{Q(3/4) - 2Q(1/2) + Q(1/4)}{Q(3/4) - Q(1/4)} \tag{20}$$

and

$$MK = \frac{Q(7/8) - Q(5/8) + Q(3/8) - Q(1/8)}{Q(6/8) - Q(2/8)}. \tag{21}$$

As a function of β, Figure 2 shows the GS and MK of the NEHTLx distribution for a few parameter choices.

Plots of GS; (a) and MK; (b) demonstrate how the NEHTLx distribution's forms are flatter than typical and strongly rely on the shape parameter values. Moreover, symmetric real-world data sets and positive and negative skewness can be modelled using the NEHTLx distribution.

3.3 *Moments*

In this section, we provide the rth moment, mean (μ_X), variance (σ_X^2), skewness ($\xi_1(X)$), kurtosis ($\xi_2(X)$) and the moment generating function (MGF) of the NEHTLx distribution. The rth moment for the Lx distribution [10] is defined by

$$\acute{\mu}_r = \lambda\delta^r B(r+1,\ \lambda - r), \tag{22}$$

where

$$B(p,\ q) = \int_0^1 w^{p-1}(1-w)^{q-1}dw, \tag{23}$$

which is the complete beta function. The first moment reduces to $\acute{\mu}_1 = \dfrac{\delta}{\lambda - 1}$ for $\lambda > 1$. As a result, we may calculate the rth moment of the NEHTLx distribution using the rth moment for the Lx distribution.

Proposition Based on (17), the rth moment of the NEHTLx distribution is defined by

$$\mu_r' = \sum_{k,\ j=0}^{\infty} \xi_{k,\ j} \int_0^{\infty} x^r g(x;\ \delta,\ \lambda(\beta+k))dx, \quad r \in \mathbb{N}. \tag{24}$$

Thus, by utilising the Lx distribution's rth moment, we get at for $r < \lambda(\beta+k)$

$$\mu_r' = \sum_{k,\ j=0}^{\infty} \xi_{k,\ j}\lambda(\beta+k)\delta^r B(r+1,\ \lambda(\beta+k) - r). \tag{25}$$

We obtain the mean of x by setting $r = 1$ in Equation (25). For $r < \lambda(\beta+k))$, the rth incomplete moment of X is provided by

$$m_r(y) = \sum_{k,\ j=0}^{\infty} \xi_{k,\ j} \int_0^{y} x^r g(x;\ \delta,\ \lambda(\beta+k))dx \ \ r \in \mathbb{N}. \tag{26}$$

and

$$m_r(y) = \sum_{k,\ j=0}^{\infty} \xi_{k,\ j} \lambda(\beta+k)\delta^r B_y(r+1,\ \lambda(\beta+k)-r), \tag{27}$$

where the incomplete beta function is denoted by $B_y(q,\ p) = \int_0^y t^{q-1}\ (1-t)^{p-1}dt$. For varying values of β, α, δ, and λ, the numerical values for μ_X, σ_X^2, $\xi_1(X)$, and $\xi_2(X)$ of the NEHTLx distribution are computed. These numerical results are presented in Table 1. The NEHTLx model is left-or right-skewed and leptokurtic (i.e., $\xi_2(X) > 3$), as Table1 illustrates. With R project programming, calculating these findings is simple. For instance, the code in Algorithm 1 can be used to compute the expectation.

Algorithm 1: Expectation algorithm

Result: Expectation.

1 Let $fx = 0,\ \boldsymbol{\psi} \subset \mathbb{R}^+$.

2 **for** $i = 2$ to length(x) **do**

3 | Compute $fx = fx + xf(x,\ \boldsymbol{\psi}) * \Delta x$

4 **end**

5 print(fx)

Table 1. Moments measures of the NEHTLx distribution for different values of the parameters β, α, δ and λ

$\boldsymbol{\psi}^{\intercal}$	μ_X	σ_X^2	$\xi_1(X)$	$\xi_2(X)$
$(\beta = 03.70,\ \alpha = 0.25,\ \delta = 1.75,\ \lambda = 02.20)$	0.7627	0.5529	2.2190	12.3453
$(\beta = 03.25,\ \alpha = 0.25,\ \delta = 1.75,\ \lambda = 03.20)$	0.5352	0.2333	1.8244	8.7703
$(\beta = 04.25,\ \alpha = 0.25,\ \delta = 2.25,\ \lambda = 03.20)$	0.5408	0.2358	1.7006	7.5684
$(\beta = 04.25,\ \alpha = 0.25,\ \delta = 4.25,\ \lambda = 04.25)$	0.7355	0.4055	1.5250	6.4145
$(\beta = 04.25,\ \alpha = 0.25,\ \delta = 4.25,\ \lambda = 01.25)$	3.5960	18.1977	3.7816	42.6721
$(\beta = 04.25,\ \alpha = 1.25,\ \delta = 4.25,\ \lambda = 01.25)$	0.7958	1.0346	4.4141	59.9953
$(\beta = 50.25,\ \alpha = 2.25,\ \delta = 3.25,\ \lambda = 30.25)$	0.0009	0	-0.1117	0.9781
$(\beta = 80.50,\ \alpha = 0.15,\ \delta = 0.75,\ \lambda = 40.50)$	0.0014	0	-0.8976	2.1914
$(\beta = 02.50,\ \alpha = 0.01,\ \delta = 1.75,\ \lambda = 150.0)$	0.0404	0.0002	-0.1309	-4.2336

3.4 *Rényi and η entropies*

A measure of uncertainty variation for a random variable X is its Rényi entropy. It is described by

$$I_\eta(X) = \frac{1}{1-\eta}\log((J_\eta(X)), \quad \eta > 0 \ \text{ and } \ \eta \neq 1, \tag{28}$$

where

$$J_\eta(X) = \int_{-\infty}^{\infty} f^\eta(x)dx. \tag{29}$$

By utilising (8), we can compose

$$f^{\eta}(x;\ \boldsymbol{\varphi}) = \left(\frac{\beta\alpha\lambda}{\delta}\right)^{\eta}\left(1+\frac{x}{\delta}\right)^{-\eta(\lambda\beta+1)}\left\{1-\bar{\alpha}\left[1-\left(1+\frac{x}{\delta}\right)^{-\lambda}\right]\right\}^{-\eta(\beta+1)}. \tag{30}$$

Following a few reductions in complexity, the Rényi entropy is expressed as

$$I_{\eta}(X) = \frac{1}{1-\eta}\log\left(\sum_{k,\ j=0}^{\infty}\binom{j}{k}\binom{-\eta(\beta+1)}{j}\frac{\beta^{\eta}\alpha^{\eta}\lambda^{\eta}(-1)^{k}(\alpha-1)^{j}}{\delta^{\eta-1}[\eta(\lambda\beta+1)+\lambda k-1]}\right). \tag{31}$$

The η-entropy, say $H_{\eta}(X)$, is given by

$$H_{\eta}(X) = \frac{1}{\eta-1}\log\left[1-J_{\eta}(X)\right],\quad \eta>0\ \text{ and }\ \eta\neq 1. \tag{32}$$

$$= \frac{1}{\eta-1}\log\left[1-\sum_{k,\ j=0}^{\infty}\binom{j}{k}\binom{-\eta(\beta+1)}{j}\frac{\beta^{\eta}\alpha^{\eta}\lambda^{\eta}(-1)^{k}(\alpha-1)^{j}}{\delta^{\eta-1}[\eta(\lambda\beta+1)+\lambda k-1]}\right]. \tag{33}$$

3.5 *Order statistics*

Let $X_1,\ \ldots,\ X_n$ be a random sample from the NEHTLx distribution, and let $X_{(1)},\ \ldots,\ X_{(n)}$ be the associated order statistics. The PDF and the CDF of the of rth order statistics, say, $X_{(i)}$ and $1\leq r\leq n$ are, respectively, given by

$$f_{X_{(i)}}(x) = \frac{n!}{(i-1)!(n-i)!}(F(x))^{i-1}(1-F(x))^{n-i}f(x) \tag{34}$$

$$= \frac{n!}{(i-1)!(n-i)!}\sum_{u=0}^{n-i}(-1)^{u}\binom{n-i}{u}(F(x))^{i-1+u}f(x), \tag{35}$$

and

$$F_{X_{(i)}}(x) = \sum_{l=k}^{n}\binom{n}{l}(F(x))^{l}(1-F(x))^{n-l}$$

$$= \sum_{l=k}^{n}\sum_{u=0}^{n-i}(-1)^{u}\binom{n}{l}\binom{n-i}{u}(F(x))^{l+u}, \tag{36}$$

for $k=1,\ 2,\ \ldots,\ n.$ From (34) and (36), it follows that the PDF and CDF of the rth order statistic of the NEHTLx are reduced to

$$f_{X_{(i)}}(x)=\frac{\beta\alpha\lambda\ x^{-(\theta+1)}\ n!}{\delta(i-1)!(n-i)!}\left(1+\frac{x}{\delta}\right)^{-(\lambda\beta+1)}\left\{1-\bar{\alpha}\left[1-\left(1+\frac{x}{\delta}\right)^{-\lambda}\right]\right\}^{-(\beta+1)} \tag{37}$$

$$\sum_{u=0}^{n-i}(-1)^{u}\binom{n-i}{u}\left[1-\left\{1+\alpha\left(\left(1+\frac{x}{\delta}\right)^{\lambda}-1\right)\right\}^{-\beta}\right]^{i+u-1} \tag{38}$$

and

$$F_{X_{(i)}}(x)=\sum_{l=k}^{n}\sum_{u=0}^{n-i}(-1)^{u}\binom{n}{l}\binom{n-i}{u}\left[1-\left\{1+\alpha\left(\left(1+\frac{x}{\delta}\right)^{\lambda}-1\right)\right\}^{-\beta}\right]^{l+u}. \tag{39}$$

3.6 *Double explanation of Lx distribution and wavelet methods*

The double distribution is essential for signal and image estimation. This section investigates the double explanation of Lx distribution using the Markov Chain Monte Carlo (MCMC) algorithm. The continuous random variable X is said to have a standard double explanation of Lx distribution with parameters $\alpha,\ \beta,\ \delta$ and λ, if its PDF is given by

$$f(x;\ \boldsymbol{\varphi})=\frac{\beta\alpha\lambda}{2\delta}\left(1+\frac{|x|}{\delta}\right)^{-\lambda\ \beta-1}\left(1-\bar{\alpha}\left(1-\left(1+\frac{|x|}{\delta}\right)^{-\lambda}\right)\right)^{-\beta-1},\quad x\in\mathbb{R}, \tag{40}$$

with mean 0, and CDF, is defined as

$$F(x;\ \boldsymbol{\varphi})=\begin{cases}\int_{-\infty}^{u}f(x;\ \boldsymbol{\varphi})dx, & \text{if}\quad u<0\\ \int_{-\infty}^{0}f(x;\ \boldsymbol{\varphi})dx+\int_{0}^{u}f(x;\ \boldsymbol{\varphi})dx, & \text{if}\quad u>0\\ 1, & \text{otherwise.}\end{cases} \tag{41}$$

The CDF will be displayed numerically using the same concept as in Algorithm 1. Hence, the same method may be used to draw the SF and HRF. The pdf is displayed as $\lambda\to\infty$, with two packs on the distribution curve, in Figure 3a. Figure 3b illustrates the cdf plot; as $\lambda\to\infty$, the CDF curve rapidly approaches one.

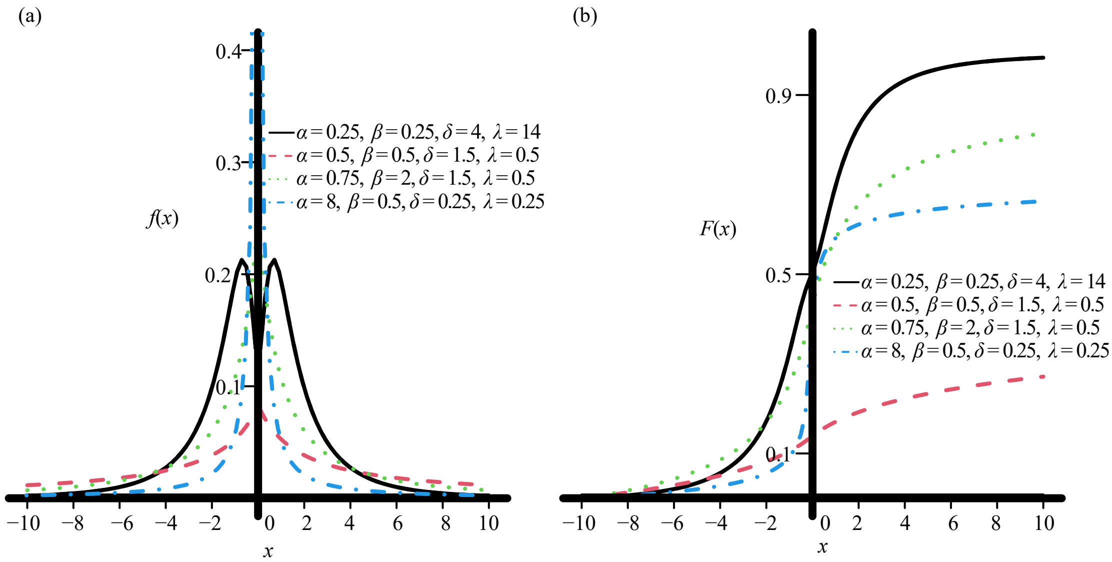

Figure 3. Plots of the PDF and CDF of the double explanation of Lx distribution for some parametric values

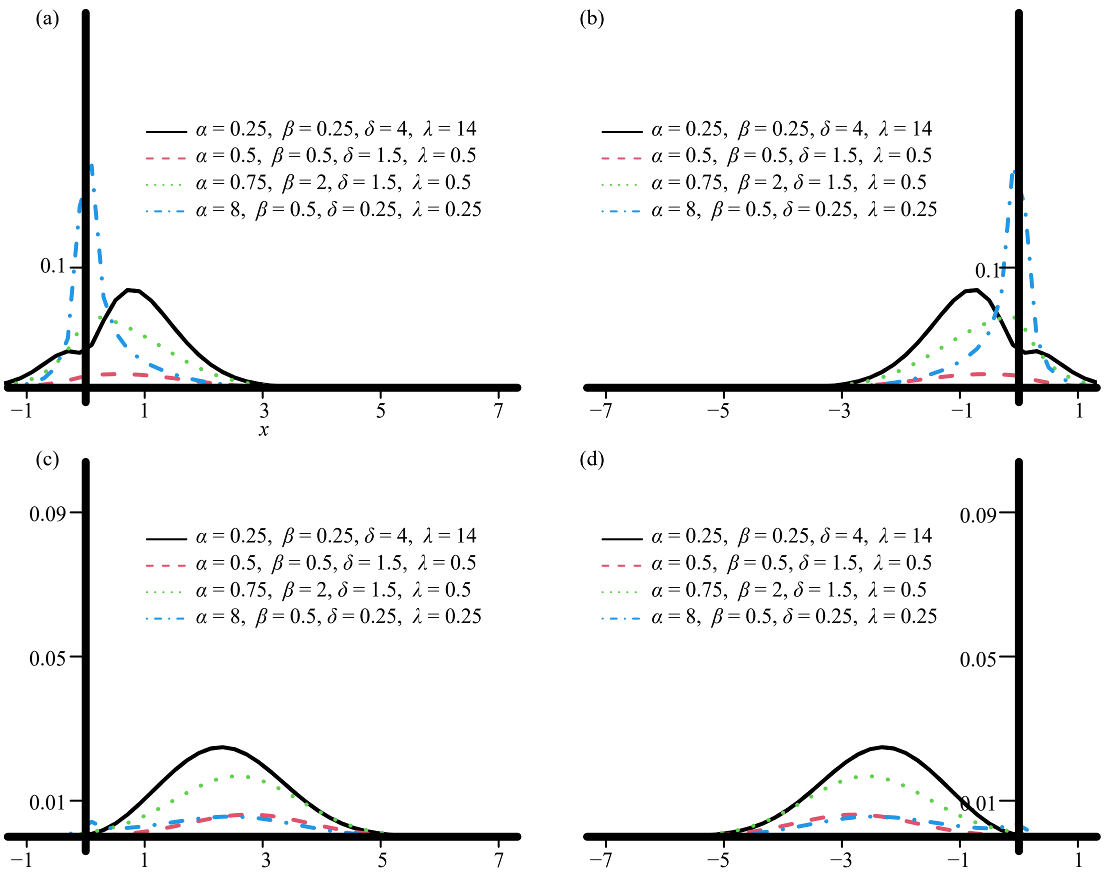

Figure 4. Plots of the likelihood in (42) for different value of the parameters to estimate the wavelet coefficients

The likelihood of the double explanation of Lx distribution for estimating wavelet coefficients is defined as

$$P(d^y;\, d^x,\, \boldsymbol{\varphi}) = \frac{\beta\alpha\lambda}{2\sqrt{2\pi}\delta} \exp\left\{ -\frac{1}{2}\left(\frac{d^y - d^x}{\sigma}\right)^2 \right\}$$

$$\times \left(1 + \frac{|d^x|}{\delta}\right)^{-\lambda\ \beta-1} \left(1 - \bar{\alpha}\left(1 - \left(1 + \frac{|d^x|}{\delta}\right)^{-\lambda}\right)\right)^{-\beta-1}, \quad d^x,\, d^y \in \mathbb{R}, \tag{42}$$

where d^x and d^y are the single of the observation, and the estimate wavelet coefficients-for more details, see [22].

Figure 4 shows the plot of the estimation of the wavelet coefficients. Note that the parameter $\lambda >> 1$ should be large for estimating the coefficients $d^x = 1$, $d^x = -1$, $d^x = 3$ and $d^x = -3$.

4. Estimation approaches

This section investigates the estimation of the NEHTLx parameters using eight different estimators: the right-tail Anderson-Darling estimators (RADE), Cramér-von Mises estimators (CVRME), weighted least-squares estimators (WLSE), maximum likelihood estimators (MLE), ordinary LSE (OLSE), maximum product of spacing estimators (MPSE), percentile estimators (PCE), and Anderson-Darling estimators (ADE).

The function is minimised by the OLSE of the NEHTLx parameters.

$$V(\boldsymbol{\psi}) = \sum_{i=1}^{n} \left[F(x_{(i)}) - \frac{i}{n+1} \right]^2. \tag{43}$$

This is another way to rewrite the equation above

$$V(\boldsymbol{\psi}) = \sum_{i=1}^{n} \left(1 - \left\{ 1 + \alpha \left[\left(1 + \frac{x_{(i)}}{\delta}\right)^{\lambda} - 1 \right] \right\}^{-\beta} - \frac{i}{n+1} \right)^2, \tag{44}$$

where $W_{(i)} = 1 + \alpha \left[\left(1 + \frac{x_{(i)}}{\delta}\right)^{\lambda} - 1 \right]$. Additionally, these estimators can be obtained by resolving the subsequent non-linear equations

$$\sum_{i=1}^{n} \left(1 - \left\{ 1 + \alpha \left[\left(1 + \frac{x_{(i)}}{\delta}\right)^{\lambda} - 1 \right] \right\}^{-\beta} - \frac{i}{n+1} \right) \Delta_s(x_{(i)}) = 0,\ s = 1,\ 2,\ 3,\ 4, \tag{45}$$

where

$$\Delta_1(x_{(i)}) = \frac{\partial F(x_{(i)})}{\partial \beta} = W_{(i)}^{-\beta} \ln W_{(i)}, \tag{46}$$

$$\Delta_2(x_{(i)}) = \frac{\partial F(x_{(i)})}{\partial \alpha} = \beta W_{(i)}^{-(\beta+1)} \left[\left(1 + \frac{x_{(i)}}{\delta}\right)^{\lambda} - 1 \right], \tag{47}$$

$$\Delta_3(x_{(i)}) = \frac{\partial F(x_{(i)})}{\partial \delta} = \frac{-\alpha\lambda\beta x_{(i)}}{\delta^2}\left(1+\frac{x_{(i)}}{\delta}\right)^{\lambda-1} W_{(i)}^{-(\beta+1)}, \tag{48}$$

and

$$\Delta_4(x_{(i)}) = \frac{\partial F(x_{(i)})}{\partial \lambda} = \alpha\beta\left(1+\frac{x_{(i)}}{\delta}\right)^{\lambda} \ln\left(1+\frac{x_{(i)}}{\delta}\right)^{\lambda} W_{(i)}^{-(\beta+1)}. \tag{49}$$

The WLSE of the NEHTLx parameters minimize

$$W(\boldsymbol{\psi}) = \sum_{i=1}^{n} \frac{(n+1)^2(n+2)}{i(n-i+1)}\left[F(x_{(i)}) - \frac{i}{n+1}\right]^2, \tag{50}$$

which follow by solving

$$\sum_{i=1}^{n} \frac{(n+1)^2(n+2)}{i(n-i+1)}\left[F(x_{(i)}) - \frac{i}{n+1}\right]\Delta_s(x_{(i)}) = 0, \quad s = 1,\ 2,\ 3,\ 4. \tag{51}$$

The MLE of the NEHTLx parameters maximize the log-likelihood, say, $\ell = \ell(\boldsymbol{\psi})$, which is given by

$$\ell = n\log(\beta) + n\log(\alpha) + n\log(\lambda) - n\log(\delta) - (\lambda\beta+1)\sum_{i=1}^{n}\log(b_i)$$

$$-(\beta+1)\sum_{i=1}^{n}\log\left\{1-\bar{\alpha}\ \left(1-b_i^{-\lambda}\right)\right\} \tag{52}$$

where $b_i = 1+\dfrac{x_i}{\delta}$, $R_i = (1-\bar{\alpha}M_i)$ and $M_i = 1-b_i^{-\lambda}$.

The likelihood equations are

$$\frac{\partial \ell}{\partial \beta} = \frac{n}{\beta} - \lambda\sum_{i=1}^{n}\log(b_i) - \sum_{i=1}^{n}\log R_i = 0 \tag{53}$$

$$\frac{\partial \ell}{\partial \alpha} = \frac{n}{\alpha} - (\beta+1)\sum_{i=1}^{n}\frac{M_i}{R_i} = 0 \tag{54}$$

$$\frac{\partial \ell}{\partial \delta} = \frac{-n}{\delta} + \frac{\lambda\beta+1}{\delta^2}\sum_{i=1}^{n} x_i\ b_i^{-1} - \frac{\bar{\alpha}\lambda(\beta+1)}{\delta^2}\sum_{i=1}^{n}\frac{x_i\ b_i^{-\lambda-1}}{R_i} = 0. \tag{55}$$

and

$$\frac{\partial \ell}{\partial \lambda}=\frac{n}{\lambda}-\beta\sum_{i=1}^{n}\log\left(b_i\right)+\bar{\alpha}\left(\beta+1\right)\sum_{i=1}^{n}\frac{b_i^{-\lambda}\log\left(b_i\right)}{R_i}=0 \tag{56}$$

Let $D_i=D_i(\boldsymbol{\psi})=F(x_{(i)})-F(x_{(i-1)})$ be the uniform spacings (for $i=1,\ \ldots,\ n+1$), where $F(x_{(0)})=0$ and $F(x_{(n+1)})=1$. Also, $\sum_{i=1}^{n+1}D_i=1$. The MPSE of the NEHTLx parameters maximize the quantity

$$H\left(\boldsymbol{\psi}\right)=\sum_{i=1}^{n+1}\log\left(D_i\right), \tag{57}$$

which can be determined from the non-linear equations

$$\sum_{i=1}^{n+1}\frac{1}{D_i}\left[\Delta_s(x_{(i)})-\Delta_s(x_{(i-1)})\right]=0,\ s=1,\ 2,\ 3,\ 4. \tag{58}$$

The Composite Relative Variance Minimization Error (CRVME) of the NEHTLx parameters minimize

$$C(\boldsymbol{\psi})=-\frac{1}{12n}+\sum_{i=1}^{n}\left[F\left(x_{(i)}\right)-\frac{2i-1}{2n}\right]^2, \tag{59}$$

which also follow by solving

$$\sum_{i=1}^{n}\left[F\left(x_{(i)}\right)-\frac{2i-1}{2n}\right]\Delta_s(x_{(i)})=0,\ s=1,\ 2,\ 3,\ 4. \tag{60}$$

The PCE method is originally suggested by [23, 24]. Let $u_i=i/\left(n+1\right)$ be an unbiased estimator of $F\left(x_{(i)}|\boldsymbol{\psi}\right)$. Then, the PCE of the NEHTLx parameters are determined by minimizing the following function

$$P(\boldsymbol{\psi})=\sum_{i=1}^{n}\left(x_{(i)}+\left\{\delta\left[\frac{\left(\bar{\alpha}-1\right)\left(1-u_i\right)^{\frac{1}{\beta}}}{\bar{\alpha}\left(1-u_i\right)^{\frac{1}{\beta}}-1}\right]^{-\frac{1}{\lambda}}-\delta\right\}\right)^2, \tag{61}$$

with respect to β, α , δ and λ. The ADE of the NEHTLx parameters minimize

$$A(\boldsymbol{\psi})=-n-\frac{1}{n}\sum_{i=1}^{n}(2i-1)\left[\log F(x_{(i)})+\log S(x_{(i)})\right], \tag{62}$$

which can be found as solutions of the following system

$$\sum_{i=1}^{n}(2i-1)\left[\frac{\Delta_s(x_{(i)})}{F(x_{(i)})}-\frac{\Delta_i(x_{(n+1-i)})}{S(x_{(n+1-i)})}\right]=0,\quad s=1,\ 2,\ 3,\ 4. \tag{63}$$

The RADE of the NEHTLx parameters minimize

$$R(\boldsymbol{\psi}) = \frac{n}{2} - 2\sum_{i=1}^{n} F(x_{(i)}) - \frac{1}{n}\sum_{i=1}^{n}(2i-1)\log S(x_{(n+1-i)}). \tag{64}$$

The RADE can also be determined from the non-linear equations

$$-2\sum_{i=1}^{n}\Delta_s(x_{(i)}) + \frac{1}{n}\sum_{i=1}^{n}(2i-1)\frac{\Delta_s(x_{(n+1-i)})}{S(x_{(n+1-i)})} = 0, \quad s = 1,\ 2,\ 3,\ 4. \tag{65}$$

5. Simulation analysis

Numerical simulations are presented in this section to investigate the performance of various estimators using the three metrics-mean squared errors (MSE),

$$\text{MSE} = \frac{1}{N}\sum_{i=1}^{N}(\widehat{\boldsymbol{\varphi}} - \boldsymbol{\varphi})^2, \tag{66}$$

also, absolute biases (|BIAS|),

$$|\text{Bias}(\widehat{\boldsymbol{\varphi}})| = \frac{1}{N}\sum_{i=1}^{N}|\widehat{\boldsymbol{\varphi}} - \boldsymbol{\varphi}|, \tag{67}$$

and mean relative errors (MRE),

$$\text{MRE} = \frac{1}{N}\sum_{i=1}^{N}|\widehat{\boldsymbol{\varphi}} - \boldsymbol{\varphi}|/\boldsymbol{\varphi}. \tag{68}$$

The QF (19) of the NEHTLx model is used to create the random samples $x_1, \ldots, x_n$. We generated $N = 5,000$ random samples of sizes, say, $n = 50,\ 150,\ 300$, and 500 for several values of its parameters $\alpha = \{0.50,\ 0.75,\ 1.00,\ 2.00,\ 4.00,\ 5.00\}$, $\beta = \{0.50,\ 0.75,\ 2.00,\ 2.75\}$, $\delta = \{1.20,\ 1.50,\ 3.00,\ 4.00,\ 6.00\}$ and $\lambda = \{0.25,\ 0.50,\ 2.00,\ 2.50,\ 3.00,\ 7.00\}$. These simulations are carried out using the `R` program (`R` Core Team, 2023, version 4.3.10). For various parameter combinations and sample sizes, the NEHTLx parameters are estimated, and the estimations of the BIAS, MSE, and MRE are also computed. The eight estimators' numerical simulations can be found in Tables 2-6. In these tables, the numbers in each row have superscripts, which refer to the ranks of each estimate among all methods, and $\sum Ranks$ represents the partial sum of the ranks. The outcomes demonstrated that all estimate techniques possessed the consistency property, meaning that for every combination of parameters, the MSE and MRE decrease as n increases. With an overall score of 74.5, Table 7 demonstrates that the RAD approach performs better than all other estimate techniques when it comes to predicting the parameters of the NEHTLx distribution. It does this by reporting the partial and overall ranks of various estimators. Moreover, simulation findings validate the superiority of the OLS and RAD techniques in NEHTLx parameter estimation.

Table 2. Simulation results for $\boldsymbol{\varphi} = (\beta = 0.75,\ \alpha = 0.5,\ \theta = 1.25,\ \lambda = 0.25)^{\intercal}$

n	Est.	Est. Par.	MLEs	LSEs	WLSEs	CRVMEs	MPSEs	PCEs	ADEs	RADEs
50	|BIAS|	$\hat{\alpha}$	$0.2059^{\{7\}}$	$0.1967^{\{6\}}$	$0.1908^{\{5\}}$	$0.1849^{\{4\}}$	$0.2282^{\{8\}}$	$0.0362^{\{1\}}$	$0.1820^{\{2\}}$	$0.1822^{\{3\}}$
		$\hat{\beta}$	$0.2192^{\{8\}}$	$0.1161^{\{5\}}$	$0.1285^{\{7\}}$	$0.1152^{\{4\}}$	$0.1022^{\{2\}}$	$0.0526^{\{1\}}$	$0.1170^{\{6\}}$	$0.1053^{\{3\}}$
		$\hat{\delta}$	$0.3965^{\{8\}}$	$0.1734^{\{4\}}$	$0.1938^{\{6\}}$	$0.1714^{\{3\}}$	$0.3825^{\{7\}}$	$0.0859^{\{1\}}$	$0.1910^{\{5\}}$	$0.1626^{\{2\}}$
		$\hat{\lambda}$	$0.0631^{\{7\}}$	$0.0442^{\{3\}}$	$0.0459^{\{5\}}$	$0.0460^{\{6\}}$	$0.0644^{\{8\}}$	$0.0310^{\{1\}}$	$0.0445^{\{4\}}$	$0.0363^{\{2\}}$
	MSE	$\hat{\alpha}$	$0.0774^{\{7\}}$	$0.0654^{\{6\}}$	$0.0604^{\{5\}}$	$0.0553^{\{4\}}$	$0.0964^{\{8\}}$	$0.0020^{\{1\}}$	$0.0550^{\{3\}}$	$0.0538^{\{2\}}$
		$\hat{\beta}$	$0.0800^{\{8\}}$	$0.0216^{\{3\}}$	$0.0262^{\{6\}}$	$0.0219^{\{4\}}$	$0.0664^{\{7\}}$	$0.0049^{\{1\}}$	$0.0231^{\{5\}}$	$0.0197^{\{2\}}$
		$\hat{\delta}$	$0.4132^{\{8\}}$	$0.0642^{\{3\}}$	$0.0859^{\{6\}}$	$0.0637^{\{2\}}$	$0.3299^{\{7\}}$	$0.0102^{\{1\}}$	$0.0838^{\{5\}}$	$0.0652^{\{4\}}$
		$\hat{\lambda}$	$0.0074^{\{8\}}$	$0.0034^{\{3\}}$	$0.0039^{\{6\}}$	$0.0038^{\{5\}}$	$0.0074^{\{7\}}$	$0.0016^{\{1\}}$	$0.0035^{\{4\}}$	$0.0024^{\{2\}}$
	MRE	$\hat{\alpha}$	$0.4119^{\{7\}}$	$0.3935^{\{6\}}$	$0.3816^{\{5\}}$	$0.3699^{\{4\}}$	$0.4564^{\{8\}}$	$0.0725^{\{1\}}$	$0.3639^{\{2\}}$	$0.3644^{\{3\}}$
		$\hat{\beta}$	$0.2923^{\{8\}}$	$0.1548^{\{4\}}$	$0.1714^{\{6\}}$	$0.1536^{\{3\}}$	$0.2768^{\{7\}}$	$0.0702^{\{1\}}$	$0.1560^{\{5\}}$	$0.1404^{\{2\}}$
		$\hat{\delta}$	$0.3172^{\{8\}}$	$0.1387^{\{4\}}$	$0.1550^{\{6\}}$	$0.1371^{\{3\}}$	$0.3060^{\{7\}}$	$0.0687^{\{1\}}$	$0.1528^{\{5\}}$	$0.1301^{\{2\}}$
		$\hat{\lambda}$	$0.2526^{\{7\}}$	$0.1771^{\{3\}}$	$0.1837^{\{5\}}$	$0.1842^{\{6\}}$	$0.2575^{\{8\}}$	$0.1241^{\{1\}}$	$0.1783^{\{4\}}$	$0.1451^{\{2\}}$
		$\sum Ranks$	$91^{\{8\}}$	$50^{\{4.5\}}$	$68^{\{6\}}$	$48^{\{3\}}$	$84^{\{7\}}$	$12^{\{1\}}$	$50^{\{4.5\}}$	$29^{\{2\}}$
150	|BIAS|	$\hat{\alpha}$	$0.1293^{\{7\}}$	$0.1159^{\{6\}}$	$0.1110^{\{3\}}$	$0.1135^{\{5\}}$	$0.1350^{\{8\}}$	$0.0350^{\{1\}}$	$0.1111^{\{4\}}$	$0.1084^{\{2\}}$
		$\hat{\beta}$	$0.1440^{\{8\}}$	$0.0802^{\{5\}}$	$0.0866^{\{6\}}$	$0.0796^{\{4\}}$	$0.1389^{\{7\}}$	$0.0485^{\{1\}}$	$0.0756^{\{3\}}$	$0.0631^{\{2\}}$
		$\hat{\delta}$	$0.3162^{\{8\}}$	$0.1290^{\{3\}}$	$0.1533^{\{5\}}$	$0.1322^{\{4\}}$	$0.2991^{\{7\}}$	$0.0827^{\{1\}}$	$0.1539^{\{6\}}$	$0.1286^{\{2\}}$
		$\hat{\lambda}$	$0.0378^{\{7\}}$	$0.0271^{\{4\}}$	$0.0274^{\{6\}}$	$0.0272^{\{5\}}$	$0.0406^{\{8\}}$	$0.0261^{\{3\}}$	$0.0248^{\{2\}}$	$0.0202^{\{1\}}$
	MSE	$\hat{\alpha}$	$0.0299^{\{7\}}$	$0.0224^{\{6\}}$	$0.0203^{\{3\}}$	$0.0210^{\{5\}}$	$0.0322^{\{8\}}$	$0.0019^{\{1\}}$	$0.0203^{\{4\}}$	$0.0198^{\{2\}}$
		$\hat{\beta}$	$0.0368^{\{8\}}$	$0.0113^{\{5\}}$	$0.0132^{\{6\}}$	$0.0110^{\{4\}}$	$0.0330^{\{7\}}$	$0.0043^{\{1\}}$	$0.0106^{\{3\}}$	$0.00798^{\{2\}}$
		$\hat{\delta}$	$0.2421^{\{8\}}$	$0.0393^{\{2\}}$	$0.0594^{\{5\}}$	$0.0428^{\{3\}}$	$0.2055^{\{7\}}$	$0.0095^{\{1\}}$	$0.0610^{\{6\}}$	$0.0514^{\{4\}}$
		$\hat{\lambda}$	$0.0026^{\{7\}}$	$0.0013^{\{5\}}$	$0.0012^{\{4\}}$	$0.0017^{\{6\}}$	$0.0030^{\{8\}}$	$0.0011^{\{3\}}$	$0.0014^{\{2\}}$	$0.0007^{\{1\}}$
	MRE	$\hat{\alpha}$	$0.2587^{\{7\}}$	$0.2319^{\{6\}}$	$0.2220^{\{3\}}$	$0.2271^{\{5\}}$	$0.2701^{\{8\}}$	$0.0700^{\{1\}}$	$0.2222^{\{4\}}$	$0.2169^{\{2\}}$
		$\hat{\beta}$	$0.1920^{\{8\}}$	$0.1070^{\{5\}}$	$0.1155^{\{6\}}$	$0.1061^{\{4\}}$	$0.1852^{\{7\}}$	$0.0647^{\{1\}}$	$0.1008^{\{3\}}$	$0.0842^{\{2\}}$
		$\hat{\delta}$	$0.2530^{\{8\}}$	$0.1032^{\{3\}}$	$0.1227^{\{5\}}$	$0.1057^{\{4\}}$	$0.2393^{\{7\}}$	$0.0662^{\{1\}}$	$0.1231^{\{6\}}$	$0.1029^{\{2\}}$
		$\hat{\lambda}$	$0.1513^{\{7\}}$	$0.1087^{\{4\}}$	$0.1096^{\{6\}}$	$0.1089^{\{5\}}$	$0.1626^{\{8\}}$	$0.1046^{\{3\}}$	$0.0994^{\{2\}}$	$0.0809^{\{1\}}$
		$\sum Ranks$	$90^{\{7.5\}}$	$54^{\{4.5\}}$	$58^{\{6\}}$	$54^{\{4.5\}}$	$90^{\{7.5\}}$	$18^{\{1\}}$	$45^{\{3\}}$	$23^{\{2\}}$
300	|BIAS|	$\hat{\alpha}$	$0.0974^{\{7\}}$	$0.0808^{\{6\}}$	$0.0799^{\{3\}}$	$0.0805^{\{5\}}$	$0.1014^{\{8\}}$	$0.0356^{\{1\}}$	$0.0800^{\{4\}}$	$0.0755^{\{2\}}$
		$\hat{\beta}$	$0.1051^{\{8\}}$	$0.0596^{\{4\}}$	$0.0662^{\{6\}}$	$0.0608^{\{5\}}$	$0.1022^{\{7\}}$	$0.0446^{\{2\}}$	$0.0577^{\{3\}}$	$0.0436^{\{1\}}$
		$\hat{\delta}$	$0.2679^{\{8\}}$	$0.1154^{\{2\}}$	$0.1342^{\{5\}}$	$0.1173^{\{4\}}$	$0.2590^{\{7\}}$	$0.0786^{\{1\}}$	$0.1359^{\{6\}}$	$0.1155^{\{3\}}$
		$\hat{\lambda}$	$0.0274^{\{7\}}$	$0.0205^{\{3\}}$	$0.0217^{\{5\}}$	$0.0212^{\{4\}}$	$0.0291^{\{8\}}$	$0.0234^{\{6\}}$	$0.0187^{\{2\}}$	$0.0153^{\{1\}}$
	MSE	$\hat{\alpha}$	$0.0164^{\{7\}}$	$0.0110^{\{6\}}$	$0.0104^{\{3\}}$	$0.0107^{\{5\}}$	$0.0176^{\{8\}}$	$0.0020^{\{1\}}$	$0.0107^{\{4\}}$	$0.0094^{\{2\}}$
		$\hat{\beta}$	$0.0207^{\{8\}}$	$0.0064^{\{4\}}$	$0.0082^{\{6\}}$	$0.0067^{\{5\}}$	$0.0192^{\{7\}}$	$0.0041^{\{2\}}$	$0.0064^{\{3\}}$	$0.0038^{\{1\}}$
		$\hat{\delta}$	$0.1672^{\{8\}}$	$0.0313^{\{2\}}$	$0.0429^{\{5\}}$	$0.0325^{\{3\}}$	$0.1519^{\{7\}}$	$0.0082^{\{1\}}$	$0.0469^{\{6\}}$	$0.0350^{\{4\}}$
		$\hat{\lambda}$	$0.0014^{\{7\}}$	$0.0007^{\{3\}}$	$0.0008^{\{5\}}$	$0.0008^{\{4\}}$	$0.0016^{\{8\}}$	$0.0009^{\{6\}}$	$0.0006^{\{2\}}$	$0.0004^{\{1\}}$
	MRE	$\hat{\alpha}$	$0.1948^{\{7\}}$	$0.1616^{\{6\}}$	$0.1598^{\{3\}}$	$0.1610^{\{5\}}$	$0.2029^{\{8\}}$	$0.0712^{\{1\}}$	$0.1600^{\{4\}}$	$0.1510^{\{2\}}$
		$\hat{\beta}$	$0.1402^{\{8\}}$	$0.0795^{\{4\}}$	$0.0882^{\{6\}}$	$0.0811^{\{5\}}$	$0.1363^{\{7\}}$	$0.0595^{\{2\}}$	$0.0769^{\{3\}}$	$0.0581^{\{1\}}$
		$\hat{\delta}$	$0.2143^{\{8\}}$	$0.0923^{\{2\}}$	$0.1074^{\{5\}}$	$0.0938^{\{4\}}$	$0.2072^{\{7\}}$	$0.0628^{\{1\}}$	$0.1087^{\{6\}}$	$0.0924^{\{3\}}$
		$\hat{\lambda}$	$0.1095^{\{7\}}$	$0.0820^{\{3\}}$	$0.0869^{\{5\}}$	$0.0851^{\{4\}}$	$0.1167^{\{8\}}$	$0.0939^{\{6\}}$	$0.0751^{\{2\}}$	$0.0615^{\{1\}}$
		$\sum Ranks$	$90^{\{7.5\}}$	$45^{\{3.5\}}$	$57^{\{6\}}$	$53^{\{5\}}$	$90^{\{7.5\}}$	$30^{\{2\}}$	$45^{\{3.5\}}$	$22^{\{1\}}$
500	|BIAS|	$\hat{\alpha}$	$0.0789^{\{7\}}$	$0.0639^{\{4\}}$	$0.0638^{\{3\}}$	$0.0644^{\{6\}}$	$0.0813^{\{8\}}$	$0.0351^{\{1\}}$	$0.0641^{\{5\}}$	$0.0595^{\{2\}}$
		$\hat{\beta}$	$0.0842^{\{8\}}$	$0.0492^{\{4\}}$	$0.0534^{\{6\}}$	$0.0494^{\{5\}}$	$0.0798^{\{7\}}$	$0.0456^{\{2\}}$	$0.0470^{\{3\}}$	$0.0348^{\{1\}}$
		$\hat{\delta}$	$0.2289^{\{8\}}$	$0.1055^{\{2\}}$	$0.1185^{\{5\}}$	$0.1088^{\{4\}}$	$0.2202^{\{7\}}$	$0.0788^{\{1\}}$	$0.1256^{\{6\}}$	$0.1060^{\{3\}}$
		$\hat{\lambda}$	$0.0225^{\{6\}}$	$0.0175^{\{4\}}$	$0.0175^{\{5\}}$	$0.0171^{\{3\}}$	$0.0230^{\{8\}}$	$0.0226^{\{7\}}$	$0.0157^{\{2\}}$	$0.0128^{\{1\}}$
	MSE	$\hat{\alpha}$	$0.0106^{\{7\}}$	$0.0069^{\{6\}}$	$0.0066^{\{3\}}$	$0.0069^{\{5\}}$	$0.0114^{\{8\}}$	$0.0020^{\{1\}}$	$0.0067^{\{4\}}$	$0.0060^{\{2\}}$
		$\hat{\beta}$	$0.0133^{\{8\}}$	$0.0045^{\{5\}}$	$0.0054^{\{6\}}$	$0.0045^{\{4\}}$	$0.0119^{\{7\}}$	$0.0044^{\{2.5\}}$	$0.0044^{\{2.5\}}$	$0.0025^{\{1\}}$
		$\hat{\delta}$	$0.1159^{\{8\}}$	$0.0252^{\{2\}}$	$0.0341^{\{5\}}$	$0.0274^{\{4\}}$	$0.1030^{\{7\}}$	$0.0082^{\{1\}}$	$0.0367^{\{6\}}$	$0.0257^{\{3\}}$
		$\hat{\lambda}$	$0.0009^{\{7\}}$	$0.0006^{\{5\}}$	$0.0005^{\{4\}}$	$0.0005^{\{3\}}$	$0.0009^{\{8\}}$	$0.0008^{\{6\}}$	$0.0004^{\{2\}}$	$0.0002^{\{1\}}$
	MRE	$\hat{\alpha}$	$0.1579^{\{7\}}$	$0.1279^{\{4\}}$	$0.1277^{\{3\}}$	$0.1289^{\{6\}}$	$0.1627^{\{8\}}$	$0.0702^{\{1\}}$	$0.1282^{\{5\}}$	$0.1191^{\{2\}}$
		$\hat{\beta}$	$0.1123^{\{8\}}$	$0.0657^{\{4\}}$	$0.0713^{\{6\}}$	$0.0659^{\{5\}}$	$0.1064^{\{7\}}$	$0.0608^{\{2\}}$	$0.0626^{\{3\}}$	$0.0464^{\{1\}}$
		$\hat{\delta}$	$0.1831^{\{8\}}$	$0.0844^{\{2\}}$	$0.0948^{\{5\}}$	$0.0870^{\{4\}}$	$0.1762^{\{7\}}$	$0.0631^{\{1\}}$	$0.1005^{\{6\}}$	$0.0848^{\{3\}}$
		$\hat{\lambda}$	$0.0900^{\{6\}}$	$0.0700^{\{4\}}$	$0.0701^{\{5\}}$	$0.0686^{\{3\}}$	$0.0919^{\{8\}}$	$0.0906^{\{7\}}$	$0.0628^{\{2\}}$	$0.0513^{\{1\}}$
		$\sum Ranks$	$88^{\{7\}}$	$46^{\{3\}}$	$56^{\{6\}}$	$52^{\{5\}}$	$90^{\{8\}}$	$32.5^{\{2\}}$	$46.5^{\{4\}}$	$21^{\{1\}}$

Table 3. Simulation results for $\boldsymbol{\varphi} = (\beta = 0.5,\ \alpha = 0.5,\ \delta = 1.25,\ \lambda = 0.5)^{\intercal}$

n	Est.	Est. Par.	MLEs	LSEs	WLSEs	CRVMEs	MPSEs	PCEs	ADEs	RADEs
50	|BIAS|	$\hat{\alpha}$	$0.1935^{\{7\}}$	$0.1881^{\{6\}}$	$0.1820^{\{5\}}$	$0.1783^{\{4\}}$	$0.2200^{\{8\}}$	$0.0547^{\{1\}}$	$0.1746^{\{2\}}$	$0.1770^{\{3\}}$
		$\hat{\beta}$	$0.1755^{\{8\}}$	$0.0734^{\{2\}}$	$0.0807^{\{5\}}$	$0.0745^{\{3\}}$	$0.0889^{\{7\}}$	$0.0337^{\{1\}}$	$0.0844^{\{6\}}$	$0.0773^{\{4\}}$
		$\hat{\delta}$	$0.2640^{\{7\}}$	$0.1394^{\{4\}}$	$0.1455^{\{6\}}$	$0.1337^{\{2\}}$	$0.2843^{\{8\}}$	$0.0963^{\{1\}}$	$0.1448^{\{5\}}$	$0.1350^{\{3\}}$
		$\hat{\lambda}$	$0.1471^{\{8\}}$	$0.0908^{\{3\}}$	$0.0958^{\{6\}}$	$0.0937^{\{4\}}$	$0.1401^{\{7\}}$	$0.0727^{\{1\}}$	$0.0938^{\{5\}}$	$0.0809^{\{2\}}$
	MSE	$\hat{\alpha}$	$0.0695^{\{7\}}$	$0.0621^{\{6\}}$	$0.0565^{\{5\}}$	$0.0517^{\{4\}}$	$0.1021^{\{8\}}$	$0.0047^{\{1\}}$	$0.0516^{\{3\}}$	$0.0510^{\{2\}}$
		$\hat{\beta}$	$0.0523^{\{8\}}$	$0.0088^{\{2\}}$	$0.0110^{\{5\}}$	$0.0094^{\{3\}}$	$0.0388^{\{7\}}$	$0.0022^{\{1\}}$	$0.0120^{\{6\}}$	$0.0103^{\{4\}}$
		$\hat{\delta}$	$0.1752^{\{7\}}$	$0.0377^{\{4\}}$	$0.0412^{\{5\}}$	$0.0349^{\{2\}}$	$0.2079^{\{8\}}$	$0.0132^{\{1\}}$	$0.0450^{\{6\}}$	$0.0351^{\{3\}}$
		$\hat{\lambda}$	$0.0374^{\{8\}}$	$0.0138^{\{3\}}$	$0.0161^{\{6\}}$	$0.0150^{\{4\}}$	$0.0331^{\{7\}}$	$0.0090^{\{1\}}$	$0.0151^{\{5\}}$	$0.0112^{\{2\}}$
	MRE	$\hat{\alpha}$	$0.3870^{\{7\}}$	$0.3762^{\{6\}}$	$0.3640^{\{5\}}$	$0.3567^{\{4\}}$	$0.4400^{\{8\}}$	$0.1095^{\{1\}}$	$0.3493^{\{2\}}$	$0.3540^{\{3\}}$
		$\hat{\beta}$	$0.3510^{\{8\}}$	$0.1468^{\{2\}}$	$0.1615^{\{5\}}$	$0.1491^{\{3\}}$	$0.3063^{\{7\}}$	$0.0674^{\{1\}}$	$0.1689^{\{6\}}$	$0.1547^{\{4\}}$
		$\hat{\delta}$	$0.2112^{\{7\}}$	$0.1115^{\{4\}}$	$0.1164^{\{6\}}$	$0.1070^{\{2\}}$	$0.2274^{\{8\}}$	$0.0770^{\{1\}}$	$0.1158^{\{5\}}$	$0.1080^{\{3\}}$
		$\hat{\lambda}$	$0.2942^{\{8\}}$	$0.1817^{\{3\}}$	$0.1916^{\{6\}}$	$0.1875^{\{4\}}$	$0.2803^{\{7\}}$	$0.1455^{\{1\}}$	$0.1877^{\{5\}}$	$0.1619^{\{2\}}$
		$\sum Ranks$	$90^{\{7.5\}}$	$45^{\{4\}}$	$65^{\{6\}}$	$39^{\{3\}}$	$90^{\{7.5\}}$	$12^{\{1\}}$	$56^{\{5\}}$	$35^{\{2\}}$
150	|BIAS|	$\hat{\alpha}$	$0.1216^{\{7\}}$	$0.1080^{\{6\}}$	$0.1050^{\{2\}}$	$0.1059^{\{5\}}$	$0.1307^{\{8\}}$	$0.0487^{\{1\}}$	$0.1050^{\{3\}}$	$0.1058^{\{4\}}$
		$\hat{\beta}$	$0.1188^{\{8\}}$	$0.0515^{\{4\}}$	$0.0559^{\{5\}}$	$0.0509^{\{3\}}$	$0.1122^{\{7\}}$	$0.0297^{\{1\}}$	$0.0564^{\{6\}}$	$0.0506^{\{2\}}$
		$\hat{\delta}$	$0.2133^{\{8\}}$	$0.0946^{\{2\}}$	$0.1027^{\{5\}}$	$0.0993^{\{4\}}$	$0.2129^{\{7\}}$	$0.0882^{\{1\}}$	$0.1039^{\{6\}}$	$0.0980^{\{3\}}$
		$\hat{\lambda}$	$0.0986^{\{7\}}$	$0.0587^{\{3\}}$	$0.0607^{\{5\}}$	$0.0586^{\{2\}}$	$0.1010^{\{8\}}$	$0.0606^{\{4\}}$	$0.0618^{\{6\}}$	$0.0518^{\{1\}}$
	MSE	$\hat{\alpha}$	$0.0271^{\{7\}}$	$0.0196^{\{6\}}$	$0.0185^{\{4\}}$	$0.0184^{\{3\}}$	$0.0340^{\{8\}}$	$0.0035^{\{1\}}$	$0.0186^{\{5\}}$	$0.0181^{\{2\}}$
		$\hat{\beta}$	$0.0239^{\{8\}}$	$0.0046^{\{4\}}$	$0.0057^{\{5\}}$	$0.0046^{\{2\}}$	$0.0205^{\{7\}}$	$0.0018^{\{1\}}$	$0.0057^{\{6\}}$	$0.0046^{\{3\}}$
		$\hat{\delta}$	$0.1177^{\{8\}}$	$0.0172^{\{2\}}$	$0.0216^{\{5\}}$	$0.0201^{\{4\}}$	$0.1122^{\{7\}}$	$0.0114^{\{1\}}$	$0.0235^{\{6\}}$	$0.0190^{\{3\}}$
		$\hat{\lambda}$	$0.0165^{\{7\}}$	$0.0061^{\{2\}}$	$0.0066^{\{5\}}$	$0.0061^{\{3\}}$	$0.0171^{\{8\}}$	$0.0063^{\{4\}}$	$0.0068^{\{6\}}$	$0.0048^{\{1\}}$
	MRE	$\hat{\alpha}$	$0.2433^{\{7\}}$	$0.2160^{\{6\}}$	$0.2100^{\{2\}}$	$0.2118^{\{5\}}$	$0.2614^{\{8\}}$	$0.0975^{\{1\}}$	$0.2101^{\{3\}}$	$0.2116^{\{4\}}$
		$\hat{\beta}$	$0.2377^{\{8\}}$	$0.1030^{\{4\}}$	$0.1118^{\{5\}}$	$0.1019^{\{3\}}$	$0.2244^{\{7\}}$	$0.0595^{\{1\}}$	$0.1128^{\{6\}}$	$0.1012^{\{2\}}$
		$\hat{\delta}$	$0.1706^{\{8\}}$	$0.0757^{\{2\}}$	$0.0822^{\{5\}}$	$0.0794^{\{4\}}$	$0.1703^{\{7\}}$	$0.0706^{\{1\}}$	$0.0831^{\{6\}}$	$0.0784^{\{3\}}$
		$\hat{\lambda}$	$0.1973^{\{7\}}$	$0.1175^{\{3\}}$	$0.1215^{\{5\}}$	$0.1172^{\{2\}}$	$0.2020^{\{8\}}$	$0.1212^{\{4\}}$	$0.1236^{\{6\}}$	$0.1037^{\{1\}}$
		$\sum Ranks$	$90^{\{7.5\}}$	$44^{\{4\}}$	$53^{\{5\}}$	$40^{\{3\}}$	$90^{\{7.5\}}$	$21^{\{1\}}$	$65^{\{6\}}$	$29^{\{2\}}$
300	|BIAS|	$\hat{\alpha}$	$0.0907^{\{7\}}$	$0.0746^{\{4\}}$	$0.0737^{\{2\}}$	$0.0744^{\{3\}}$	$0.0956^{\{8\}}$	$0.0447^{\{1\}}$	$0.0755^{\{6\}}$	$0.0747^{\{5\}}$
		$\hat{\beta}$	$0.0928^{\{8\}}$	$0.0402^{\{4\}}$	$0.0432^{\{5\}}$	$0.0395^{\{2\}}$	$0.0889^{\{7\}}$	$0.0271^{\{1\}}$	$0.0441^{\{6\}}$	$0.0396^{\{3\}}$
		$\hat{\delta}$	$0.1819^{\{8\}}$	$0.0832^{\{1\}}$	$0.0893^{\{5\}}$	$0.0855^{\{3\}}$	$0.1737^{\{7\}}$	$0.0846^{\{2\}}$	$0.0916^{\{6\}}$	$0.0869^{\{4\}}$
		$\hat{\lambda}$	$0.0780^{\{7\}}$	$0.0459^{\{2\}}$	$0.0480^{\{4\}}$	$0.0469^{\{3\}}$	$0.0808^{\{8\}}$	$0.0544^{\{6\}}$	$0.0483^{\{5\}}$	$0.0418^{\{1\}}$
	MSE	$\hat{\alpha}$	$0.0153^{\{7\}}$	$0.0094^{\{5\}}$	$0.0089^{\{2\}}$	$0.0091^{\{4\}}$	$0.0179^{\{8\}}$	$0.0029^{\{1\}}$	$0.0094^{\{6\}}$	$0.0091^{\{3\}}$
		$\hat{\beta}$	$0.0148^{\{8\}}$	$0.0030^{\{4\}}$	$0.0035^{\{5\}}$	$0.0029^{\{3\}}$	$0.0133^{\{7\}}$	$0.0015^{\{1\}}$	$0.0036^{\{6\}}$	$0.0029^{\{2\}}$
		$\hat{\delta}$	$0.0832^{\{8\}}$	$0.0137^{\{2\}}$	$0.0164^{\{5\}}$	$0.0143^{\{3\}}$	$0.0761^{\{7\}}$	$0.0102^{\{1\}}$	$0.0182^{\{6\}}$	$0.0149^{\{4\}}$
		$\hat{\lambda}$	$0.0104^{\{7\}}$	$0.0037^{\{2\}}$	$0.0042^{\{5\}}$	$0.0038^{\{3\}}$	$0.0115^{\{8\}}$	$0.0052^{\{6\}}$	$0.0041^{\{4\}}$	$0.0031^{\{1\}}$
	MRE	$\hat{\alpha}$	$0.1815^{\{7\}}$	$0.1492^{\{4\}}$	$0.1474^{\{2\}}$	$0.1488^{\{3\}}$	$0.1913^{\{8\}}$	$0.0895^{\{1\}}$	$0.1511^{\{6\}}$	$0.1495^{\{5\}}$
		$\hat{\beta}$	$0.1857^{\{8\}}$	$0.0805^{\{4\}}$	$0.0865^{\{5\}}$	$0.0790^{\{2\}}$	$0.1779^{\{7\}}$	$0.0542^{\{1\}}$	$0.0882^{\{6\}}$	$0.0793^{\{3\}}$
		$\hat{\delta}$	$0.1455^{\{8\}}$	$0.0666^{\{1\}}$	$0.0715^{\{5\}}$	$0.0684^{\{3\}}$	$0.1390^{\{7\}}$	$0.0677^{\{2\}}$	$0.0733^{\{6\}}$	$0.0695^{\{4\}}$
		$\hat{\lambda}$	$0.1560^{\{7\}}$	$0.0918^{\{2\}}$	$0.0961^{\{4\}}$	$0.0939^{\{3\}}$	$0.1617^{\{8\}}$	$0.1089^{\{6\}}$	$0.0967^{\{5\}}$	$0.0837^{\{1\}}$
		$\sum Ranks$	$90^{\{7.5\}}$	$35^{\{2.5\}}$	$49^{\{5\}}$	$35^{\{2.5\}}$	$90^{\{7.5\}}$	$29^{\{1\}}$	$68^{\{6\}}$	$36^{\{4\}}$
500	|BIAS|	$\hat{\alpha}$	$0.0737^{\{7\}}$	$0.0582^{\{2\}}$	$0.0588^{\{4\}}$	$0.0584^{\{3\}}$	$0.0766^{\{8\}}$	$0.0436^{\{1\}}$	$0.0589^{\{5\}}$	$0.0599^{\{6\}}$
		$\hat{\beta}$	$0.0783^{\{8\}}$	$0.0345^{\{4\}}$	$0.0372^{\{5\}}$	$0.0342^{\{3\}}$	$0.0759^{\{7\}}$	$0.0259^{\{1\}}$	$0.0381^{\{6\}}$	$0.0338^{\{2\}}$
		$\hat{\delta}$	$0.1588^{\{8\}}$	$0.0764^{\{1\}}$	$0.0838^{\{5\}}$	$0.0767^{\{2\}}$	$0.1553^{\{7\}}$	$0.0829^{\{4\}}$	$0.0841^{\{6\}}$	$0.0812^{\{3\}}$
		$\hat{\lambda}$	$0.0663^{\{7\}}$	$0.0409^{\{4\}}$	$0.0399^{\{2\}}$	$0.0407^{\{3\}}$	$0.0676^{\{8\}}$	$0.0509^{\{6\}}$	$0.0416^{\{5\}}$	$0.0356^{\{1\}}$
	MSE	$\hat{\alpha}$	$0.0098^{\{7\}}$	$0.0056^{\{3\}}$	$0.0056^{\{4\}}$	$0.0056^{\{2\}}$	$0.0110^{\{8\}}$	$0.0027^{\{1\}}$	$0.0057^{\{5\}}$	$0.0059^{\{6\}}$
		$\hat{\beta}$	$0.0104^{\{8\}}$	$0.0022^{\{4\}}$	$0.0027^{\{5\}}$	$0.0022^{\{3\}}$	$0.0097^{\{7\}}$	$0.0014^{\{1\}}$	$0.0028^{\{6\}}$	$0.0021^{\{2\}}$
		$\hat{\delta}$	$0.0600^{\{8\}}$	$0.0114^{\{3\}}$	$0.0155^{\{6\}}$	$0.0111^{\{2\}}$	$0.0586^{\{7\}}$	$0.0101^{\{1\}}$	$0.0145^{\{5\}}$	$0.0125^{\{4\}}$
		$\hat{\lambda}$	$0.0078^{\{7\}}$	$0.0029^{\{2\}}$	$0.0029^{\{3\}}$	$0.0029^{\{4\}}$	$0.0079^{\{8\}}$	$0.0044^{\{6\}}$	$0.0031^{\{5\}}$	$0.0022^{\{1\}}$
	MRE	$\hat{\alpha}$	$0.1474^{\{7\}}$	$0.1163^{\{2\}}$	$0.1176^{\{4\}}$	$0.1169^{\{3\}}$	$0.1533^{\{8\}}$	$0.0873^{\{1\}}$	$0.1179^{\{5\}}$	$0.1199^{\{6\}}$
		$\hat{\beta}$	$0.1566^{\{8\}}$	$0.0690^{\{4\}}$	$0.0744^{\{5\}}$	$0.0685^{\{3\}}$	$0.1518^{\{7\}}$	$0.0518^{\{1\}}$	$0.0763^{\{6\}}$	$0.0676^{\{2\}}$
		$\hat{\delta}$	$0.1271^{\{8\}}$	$0.0611^{\{1\}}$	$0.0671^{\{5\}}$	$0.0614^{\{2\}}$	$0.1242^{\{7\}}$	$0.0663^{\{4\}}$	$0.0673^{\{6\}}$	$0.0649^{\{3\}}$
		$\hat{\lambda}$	$0.1325^{\{7\}}$	$0.0819^{\{4\}}$	$0.0799^{\{2\}}$	$0.0815^{\{3\}}$	$0.1353^{\{8\}}$	$0.1018^{\{6\}}$	$0.0833^{\{5\}}$	$0.0713^{\{1\}}$
		$\sum Ranks$	$90^{\{7.5\}}$	$34^{\{3\}}$	$50^{\{5\}}$	$33^{\{1.5\}}$	$90^{\{7.5\}}$	$33^{\{1.5\}}$	$65^{\{6\}}$	$37^{\{4\}}$

Table 4. Simulation results for $\boldsymbol{\varphi} = (\beta = 2,\ \alpha = 0.75,\ \delta = 1.5,\ \lambda = 2.5)^{\intercal}$

n	Est.	Est. Par.	MLEs	LSEs	WLSEs	CRVMEs	MPSEs	PCEs	ADEs	RADEs
50	|BIAS|	$\hat{\alpha}$	$0.3824^{\{3\}}$	$0.4000^{\{5\}}$	$0.4072^{\{6\}}$	$0.3706^{\{2\}}$	$0.4839^{\{7\}}$	$0.5285^{\{8\}}$	$0.3936^{\{4\}}$	$0.3629^{\{1\}}$
		$\hat{\beta}$	$0.4527^{\{8\}}$	$0.3294^{\{5\}}$	$0.3366^{\{6\}}$	$0.3152^{\{2\}}$	$0.2386^{\{1\}}$	$0.3982^{\{7\}}$	$0.3291^{\{4\}}$	$0.3251^{\{3\}}$
		$\hat{\delta}$	$0.2802^{\{8\}}$	$0.2077^{\{3\}}$	$0.2121^{\{5\}}$	$0.2066^{\{2\}}$	$0.2626^{\{6\}}$	$0.2768^{\{7\}}$	$0.2087^{\{4\}}$	$0.1974^{\{1\}}$
		$\hat{\lambda}$	$0.4531^{\{8\}}$	$0.3817^{\{2\}}$	$0.4025^{\{4\}}$	$0.4055^{\{5\}}$	$0.4393^{\{7\}}$	$0.4090^{\{6\}}$	$0.3961^{\{3\}}$	$0.3773^{\{1\}}$
	MSE	$\hat{\alpha}$	$0.2416^{\{2\}}$	$0.2985^{\{5\}}$	$0.3059^{\{6\}}$	$0.2469^{\{3\}}$	$0.4233^{\{7\}}$	$0.5376^{\{8\}}$	$0.2914^{\{4\}}$	$0.2339^{\{1\}}$
		$\hat{\beta}$	$0.3454^{\{8\}}$	$0.1825^{\{3\}}$	$0.1910^{\{5\}}$	$0.1659^{\{1\}}$	$0.3148^{\{7\}}$	$0.2540^{\{6\}}$	$0.1855^{\{4\}}$	$0.1744^{\{2\}}$
		$\hat{\delta}$	$0.1651^{\{7\}}$	$0.0947^{\{3\}}$	$0.0968^{\{4\}}$	$0.0928^{\{2\}}$	$0.1342^{\{6\}}$	$0.1769^{\{8\}}$	$0.1028^{\{5\}}$	$0.0857^{\{1\}}$
		$\hat{\lambda}$	$0.3812^{\{8\}}$	$0.2628^{\{2\}}$	$0.2983^{\{4\}}$	$0.2996^{\{5\}}$	$0.3431^{\{7\}}$	$0.3010^{\{6\}}$	$0.2917^{\{3\}}$	$0.2628^{\{1\}}$
	MRE	$\hat{\alpha}$	$0.5099^{\{3\}}$	$0.5334^{\{5\}}$	$0.5429^{\{6\}}$	$0.4942^{\{2\}}$	$0.6452^{\{7\}}$	$0.7047^{\{8\}}$	$0.5249^{\{4\}}$	$0.4838^{\{1\}}$
		$\hat{\beta}$	$0.2263^{\{8\}}$	$0.1647^{\{4\}}$	$0.1683^{\{5\}}$	$0.1576^{\{1\}}$	$0.2232^{\{7\}}$	$0.1991^{\{6\}}$	$0.1645^{\{3\}}$	$0.1625^{\{2\}}$
		$\hat{\delta}$	$0.1868^{\{8\}}$	$0.1385^{\{3\}}$	$0.1414^{\{5\}}$	$0.1377^{\{2\}}$	$0.1750^{\{6\}}$	$0.1845^{\{7\}}$	$0.1391^{\{4\}}$	$0.1316^{\{1\}}$
		$\hat{\lambda}$	$0.1812^{\{8\}}$	$0.1527^{\{2\}}$	$0.1610^{\{4\}}$	$0.1622^{\{5\}}$	$0.1757^{\{7\}}$	$0.1636^{\{6\}}$	$0.1584^{\{3\}}$	$0.1509^{\{1\}}$
		$\sum Ranks$	$79^{\{7\}}$	$42^{\{3\}}$	$60^{\{5\}}$	$32^{\{2\}}$	$75^{\{6\}}$	$83^{\{8\}}$	$45^{\{4\}}$	$16^{\{1\}}$
150	|BIAS|	$\hat{\alpha}$	$0.2322^{\{6\}}$	$0.2307^{\{5\}}$	$0.2234^{\{2\}}$	$0.2257^{\{3\}}$	$0.2612^{\{7\}}$	$0.4076^{\{8\}}$	$0.2290^{\{4\}}$	$0.2144^{\{1\}}$
		$\hat{\beta}$	$0.3112^{\{7\}}$	$0.2320^{\{4\}}$	$0.2293^{\{2\}}$	$0.2298^{\{3\}}$	$0.3104^{\{6\}}$	$0.3240^{\{8\}}$	$0.2365^{\{5\}}$	$0.2273^{\{1\}}$
		$\hat{\delta}$	$0.2044^{\{7\}}$	$0.1313^{\{5\}}$	$0.1244^{\{2\}}$	$0.1257^{\{3\}}$	$0.2008^{\{6\}}$	$0.2151^{\{8\}}$	$0.1279^{\{4\}}$	$0.1227^{\{1\}}$
		$\hat{\lambda}$	$0.3012^{\{8\}}$	$0.2774^{\{4\}}$	$0.2715^{\{2\}}$	$0.2784^{\{5\}}$	$0.2909^{\{7\}}$	$0.2903^{\{6\}}$	$0.2739^{\{3\}}$	$0.2486^{\{1\}}$
	MSE	$\hat{\alpha}$	$0.0878^{\{2\}}$	$0.0963^{\{6\}}$	$0.0886^{\{3\}}$	$0.0904^{\{4\}}$	$0.1217^{\{7\}}$	$0.3521^{\{8\}}$	$0.0946^{\{5\}}$	$0.0822^{\{1\}}$
		$\hat{\beta}$	$0.1711^{\{7\}}$	$0.0924^{\{4\}}$	$0.0909^{\{3\}}$	$0.0897^{\{2\}}$	$0.1595^{\{6\}}$	$0.1793^{\{8\}}$	$0.0972^{\{5\}}$	$0.0882^{\{1\}}$
		$\hat{\delta}$	$0.1011^{\{7\}}$	$0.0405^{\{5\}}$	$0.0325^{\{1\}}$	$0.0365^{\{3\}}$	$0.0861^{\{6\}}$	$0.1210^{\{8\}}$	$0.0394^{\{4\}}$	$0.0351^{\{2\}}$
		$\hat{\lambda}$	$0.1771^{\{8\}}$	$0.1448^{\{3\}}$	$0.1429^{\{2\}}$	$0.1494^{\{5\}}$	$0.1673^{\{6\}}$	$0.1681^{\{7\}}$	$0.1474^{\{4\}}$	$0.1227^{\{1\}}$
	MRE	$\hat{\alpha}$	$0.3096^{\{6\}}$	$0.3076^{\{5\}}$	$0.2980^{\{2\}}$	$0.3010^{\{3\}}$	$0.3486^{\{7\}}$	$0.5436^{\{8\}}$	$0.3055^{\{4\}}$	$0.2859^{\{1\}}$
		$\hat{\beta}$	$0.1556^{\{7\}}$	$0.1160^{\{4\}}$	$0.1147^{\{2\}}$	$0.1149^{\{3\}}$	$0.1552^{\{6\}}$	$0.1620^{\{8\}}$	$0.1182^{\{5\}}$	$0.1136^{\{1\}}$
		$\hat{\delta}$	$0.1363^{\{7\}}$	$0.0876^{\{5\}}$	$0.0830^{\{2\}}$	$0.0838^{\{3\}}$	$0.1339^{\{6\}}$	$0.1434^{\{8\}}$	$0.0853^{\{4\}}$	$0.0819^{\{1\}}$
		$\hat{\lambda}$	$0.1205^{\{8\}}$	$0.1109^{\{4\}}$	$0.1086^{\{2\}}$	$0.1114^{\{5\}}$	$0.1164^{\{7\}}$	$0.1161^{\{6\}}$	$0.1096^{\{3\}}$	$0.0995^{\{1\}}$
		$\sum Ranks$	$80^{\{7\}}$	$54^{\{5\}}$	$25^{\{2\}}$	$42^{\{3\}}$	$77^{\{6\}}$	$91^{\{8\}}$	$50^{\{4\}}$	$13^{\{1\}}$
300	|BIAS|	$\hat{\alpha}$	$0.16261^{\{6\}}$	$0.15628^{\{4\}}$	$0.15612^{\{2\}}$	$0.15633^{\{5\}}$	$0.18416^{\{7\}}$	$0.34181^{\{8\}}$	$0.15620^{\{3\}}$	$0.14420^{\{1\}}$
		$\hat{\beta}$	$0.22806^{\{6\}}$	$0.18346^{\{5\}}$	$0.17575^{\{2\}}$	$0.18330^{\{4\}}$	$0.23866^{\{7\}}$	$0.28088^{\{8\}}$	$0.18184^{\{3\}}$	$0.17178^{\{1\}}$
		$\hat{\delta}$	$0.17006^{\{6\}}$	$0.09357^{\{1\}}$	$0.09568^{\{4\}}$	$0.09823^{\{5\}}$	$0.17191^{\{7\}}$	$0.18296^{\{8\}}$	$0.09537^{\{2\}}$	$0.09555^{\{3\}}$
		$\hat{\lambda}$	$0.22384^{\{7\}}$	$0.20558^{\{4\}}$	$0.20115^{\{2\}}$	$0.22278^{\{6\}}$	$0.21761^{\{5\}}$	$0.24441^{\{8\}}$	$0.20232^{\{3\}}$	$0.18778^{\{1\}}$
	MSE	$\hat{\alpha}$	$0.0453^{\{6\}}$	$0.0437^{\{5\}}$	$0.0423^{\{2\}}$	$0.0432^{\{3\}}$	$0.0601^{\{7\}}$	$0.2859^{\{8\}}$	$0.0436^{\{4\}}$	$0.0360^{\{1\}}$
		$\hat{\beta}$	$0.0949^{\{6\}}$	$0.0579^{\{4\}}$	$0.0534^{\{2\}}$	$0.0576^{\{3\}}$	$0.1002^{\{7\}}$	$0.1401^{\{8\}}$	$0.0584^{\{5\}}$	$0.0534^{\{1\}}$
		$\hat{\delta}$	$0.0702^{\{7\}}$	$0.0184^{\{1\}}$	$0.0196^{\{3\}}$	$0.0211^{\{5\}}$	$0.0674^{\{6\}}$	$0.0933^{\{8\}}$	$0.0194^{\{2\}}$	$0.0198^{\{4\}}$
		$\hat{\lambda}$	$0.0982^{\{6\}}$	$0.0842^{\{4\}}$	$0.0824^{\{3\}}$	$0.0992^{\{7\}}$	$0.0972^{\{5\}}$	$0.1228^{\{8\}}$	$0.0821^{\{2\}}$	$0.0696^{\{1\}}$
	MRE	$\hat{\alpha}$	$0.2168^{\{6\}}$	$0.2084^{\{4\}}$	$0.2082^{\{2\}}$	$0.2084^{\{5\}}$	$0.2456^{\{7\}}$	$0.4558^{\{8\}}$	$0.2083^{\{3\}}$	$0.1923^{\{1\}}$
		$\hat{\beta}$	$0.1140^{\{6\}}$	$0.0917^{\{5\}}$	$0.0879^{\{2\}}$	$0.0917^{\{4\}}$	$0.1193^{\{7\}}$	$0.1404^{\{8\}}$	$0.0909^{\{3\}}$	$0.0858^{\{1\}}$
		$\hat{\delta}$	$0.1134^{\{6\}}$	$0.0624^{\{1\}}$	$0.0638^{\{4\}}$	$0.0655^{\{5\}}$	$0.1146^{\{7\}}$	$0.1219^{\{8\}}$	$0.0636^{\{2\}}$	$0.0637^{\{3\}}$
		$\hat{\lambda}$	$0.0895^{\{7\}}$	$0.0822^{\{4\}}$	$0.0805^{\{2\}}$	$0.0891^{\{6\}}$	$0.0872^{\{5\}}$	$0.0978^{\{8\}}$	$0.0809^{\{3\}}$	$0.0751^{\{1\}}$
		$\sum Ranks$	$75^{\{6\}}$	$42^{\{4\}}$	$30^{\{2\}}$	$58^{\{5\}}$	$77^{\{7\}}$	$96^{\{8\}}$	$35^{\{3\}}$	$19^{\{1\}}$
500	|BIAS|	$\hat{\alpha}$	$0.1286^{\{6\}}$	$0.1214^{\{4\}}$	$0.1179^{\{2\}}$	$0.1217^{\{5\}}$	$0.1386^{\{7\}}$	$0.2766^{\{8\}}$	$0.1188^{\{3\}}$	$0.1123^{\{1\}}$
		$\hat{\beta}$	$0.1837^{\{6\}}$	$0.1504^{\{4\}}$	$0.1449^{\{3\}}$	$0.1526^{\{5\}}$	$0.1929^{\{7\}}$	$0.2513^{\{8\}}$	$0.1422^{\{2\}}$	$0.1409^{\{1\}}$
		$\hat{\delta}$	$0.1502^{\{7\}}$	$0.0799^{\{4\}}$	$0.0789^{\{1\}}$	$0.0794^{\{3\}}$	$0.1484^{\{6\}}$	$0.1524^{\{8\}}$	$0.0790^{\{2\}}$	$0.0833^{\{5\}}$
		$\hat{\lambda}$	$0.1823^{\{7\}}$	$0.1714^{\{4\}}$	$0.1654^{\{3\}}$	$0.1764^{\{5\}}$	$0.1765^{\{6\}}$	$0.2137^{\{8\}}$	$0.1644^{\{2\}}$	$0.1517^{\{1\}}$
	MSE	$\hat{\alpha}$	$0.0273^{\{6\}}$	$0.0259^{\{5\}}$	$0.0239^{\{2\}}$	$0.0256^{\{4\}}$	$0.0337^{\{7\}}$	$0.1812^{\{8\}}$	$0.0248^{\{3\}}$	$0.0225^{\{1\}}$
		$\hat{\beta}$	$0.0613^{\{6\}}$	$0.0391^{\{4\}}$	$0.0361^{\{2\}}$	$0.0407^{\{5\}}$	$0.0671^{\{7\}}$	$0.1138^{\{8\}}$	$0.0355^{\{1\}}$	$0.0371^{\{3\}}$
		$\hat{\delta}$	$0.0564^{\{7\}}$	$0.0132^{\{4\}}$	$0.0129^{\{3\}}$	$0.0126^{\{1\}}$	$0.0501^{\{6\}}$	$0.0603^{\{8\}}$	$0.0128^{\{2\}}$	$0.0143^{\{5\}}$
		$\hat{\lambda}$	$0.0657^{\{7\}}$	$0.0586^{\{4\}}$	$0.0544^{\{3\}}$	$0.0623^{\{5\}}$	$0.0632^{\{6\}}$	$0.0985^{\{8\}}$	$0.0537^{\{2\}}$	$0.0457^{\{1\}}$
	MRE	$\hat{\alpha}$	$0.1715^{\{6\}}$	$0.1618^{\{4\}}$	$0.1573^{\{2\}}$	$0.1622^{\{5\}}$	$0.1848^{\{7\}}$	$0.3688^{\{8\}}$	$0.1585^{\{3\}}$	$0.1498^{\{1\}}$
		$\hat{\beta}$	$0.0919^{\{6\}}$	$0.0752^{\{4\}}$	$0.0725^{\{3\}}$	$0.0763^{\{5\}}$	$0.0965^{\{7\}}$	$0.1257^{\{8\}}$	$0.0711^{\{2\}}$	$0.0705^{\{1\}}$
		$\hat{\delta}$	$0.1001^{\{7\}}$	$0.0533^{\{4\}}$	$0.0527^{\{1\}}$	$0.0529^{\{3\}}$	$0.0989^{\{6\}}$	$0.1016^{\{8\}}$	$0.0527^{\{2\}}$	$0.0555^{\{5\}}$
		$\hat{\lambda}$	$0.0729^{\{7\}}$	$0.0686^{\{4\}}$	$0.0662^{\{3\}}$	$0.07054^{\{5\}}$	$0.0706^{\{6\}}$	$0.0855^{\{8\}}$	$0.0658^{\{2\}}$	$0.0607^{\{1\}}$
		$\sum Ranks$	$78^{\{6.5\}}$	$49^{\{4\}}$	$28^{\{3\}}$	$51^{\{5\}}$	$78^{\{6.5\}}$	$96^{\{8\}}$	$26^{\{1.5\}}$	$26^{\{1.5\}}$

Table 5. Simulation results for $\boldsymbol{\varphi} = (\beta = 2,\ \alpha = 2,\ \delta = 3,\ \lambda = 2)^{\intercal}$

n	Est.	Est. Par.	MLEs	LSEs	WLSEs	CRVMEs	MPSEs	PCEs	ADEs	RADEs
50	|BIAS|	$\hat{\alpha}$	$0.8245^{\{6\}}$	$0.7630^{\{2\}}$	$0.7973^{\{5\}}$	$0.7241^{\{1\}}$	$0.9866^{\{7\}}$	$1.1238^{\{8\}}$	$0.7802^{\{4\}}$	$0.7636^{\{3\}}$
		$\hat{\beta}$	$0.6650^{\{8\}}$	$0.5625^{\{5\}}$	$0.5710^{\{6\}}$	$0.5578^{\{3\}}$	$0.3161^{\{1\}}$	$0.5592^{\{4\}}$	$0.5744^{\{7\}}$	$0.5302^{\{2\}}$
		$\hat{\delta}$	$0.4195^{\{6\}}$	$0.3700^{\{5\}}$	$0.3650^{\{4\}}$	$0.3578^{\{2\}}$	$0.4756^{\{8\}}$	$0.4415^{\{7\}}$	$0.3637^{\{3\}}$	$0.3309^{\{1\}}$
		$\hat{\lambda}$	$0.6878^{\{8\}}$	$0.3354^{\{1\}}$	$0.3771^{\{5\}}$	$0.3492^{\{2\}}$	$0.5876^{\{7\}}$	$0.4438^{\{6\}}$	$0.3684^{\{4\}}$	$0.3637^{\{3\}}$
	MSE	$\hat{\alpha}$	$1.0035^{\{6\}}$	$0.9571^{\{3\}}$	$0.9990^{\{5\}}$	$0.8266^{\{1\}}$	$1.5486^{\{7\}}$	$2.0740^{\{8\}}$	$0.9640^{\{4\}}$	$0.9126^{\{2\}}$
		$\hat{\beta}$	$0.6975^{\{8\}}$	$0.4541^{\{3\}}$	$0.4818^{\{5\}}$	$0.4580^{\{4\}}$	$0.5514^{\{7\}}$	$0.4536^{\{2\}}$	$0.4927^{\{6\}}$	$0.4188^{\{1\}}$
		$\hat{\delta}$	$0.3289^{\{6\}}$	$0.2894^{\{5\}}$	$0.2746^{\{2\}}$	$0.2747^{\{3\}}$	$0.4102^{\{7\}}$	$0.4171^{\{8\}}$	$0.2774^{\{4\}}$	$0.2147^{\{1\}}$
		$\hat{\lambda}$	$0.7257^{\{8\}}$	$0.2025^{\{1\}}$	$0.2600^{\{5\}}$	$0.2234^{\{2\}}$	$0.5239^{\{7\}}$	$0.3166^{\{6\}}$	$0.2446^{\{4\}}$	$0.2383^{\{3\}}$
	MRE	$\hat{\alpha}$	$0.4122^{\{6\}}$	$0.3815^{\{2\}}$	$0.3986^{\{5\}}$	$0.3620^{\{1\}}$	$0.4933^{\{7\}}$	$0.5619^{\{8\}}$	$0.3901^{\{4\}}$	$0.3818^{\{3\}}$
		$\hat{\beta}$	$0.3325^{\{8\}}$	$0.2812^{\{4\}}$	$0.2855^{\{5\}}$	$0.2789^{\{2\}}$	$0.3056^{\{7\}}$	$0.2796^{\{3\}}$	$0.2872^{\{6\}}$	$0.2651^{\{1\}}$
		$\hat{\delta}$	$0.1398^{\{6\}}$	$0.1233^{\{5\}}$	$0.1216^{\{4\}}$	$0.1192^{\{2\}}$	$0.1585^{\{8\}}$	$0.1472^{\{7\}}$	$0.1212^{\{3\}}$	$0.1103^{\{1\}}$
		$\hat{\lambda}$	$0.3439^{\{8\}}$	$0.1677^{\{1\}}$	$0.1885^{\{5\}}$	$0.1746^{\{2\}}$	$0.2938^{\{7\}}$	$0.2219^{\{6\}}$	$0.1842^{\{4\}}$	$0.1818^{\{3\}}$
		$\sum Ranks$	$84^{\{8\}}$	$37^{\{3\}}$	$56^{\{5\}}$	$25^{\{2\}}$	$80^{\{7\}}$	$73^{\{6\}}$	$53^{\{4\}}$	$24^{\{1\}}$
150	|BIAS|	$\hat{\alpha}$	$0.5219^{\{6\}}$	$0.5154^{\{4\}}$	$0.5117^{\{3\}}$	$0.4981^{\{1\}}$	$0.6017^{\{7\}}$	$0.9508^{\{8\}}$	$0.5203^{\{5\}}$	$0.5012^{\{2\}}$
		$\hat{\beta}$	$0.4345^{\{8\}}$	$0.4162^{\{6\}}$	$0.4112^{\{4\}}$	$0.4087^{\{3\}}$	$0.4231^{\{7\}}$	$0.3982^{\{2\}}$	$0.4152^{\{5\}}$	$0.3688^{\{1\}}$
		$\hat{\delta}$	$0.2673^{\{6\}}$	$0.2405^{\{4\}}$	$0.2349^{\{2\}}$	$0.2411^{\{5\}}$	$0.2796^{\{7\}}$	$0.3802^{\{8\}}$	$0.2392^{\{3\}}$	$0.2189^{\{1\}}$
		$\hat{\lambda}$	$0.4695^{\{8\}}$	$0.2592^{\{2\}}$	$0.2697^{\{5\}}$	$0.2651^{\{3\}}$	$0.4386^{\{7\}}$	$0.3832^{\{6\}}$	$0.2665^{\{4\}}$	$0.2493^{\{1\}}$
	MSE	$\hat{\alpha}$	$0.4286^{\{4\}}$	$0.4479^{\{6\}}$	$0.4281^{\{3\}}$	$0.4017^{\{1\}}$	$0.6030^{\{7\}}$	$1.6829^{\{8\}}$	$0.4436^{\{5\}}$	$0.4108^{\{2\}}$
		$\hat{\beta}$	$0.3061^{\{8\}}$	$0.2624^{\{5\}}$	$0.2600^{\{4\}}$	$0.2558^{\{3\}}$	$0.2778^{\{7\}}$	$0.2508^{\{2\}}$	$0.2698^{\{6\}}$	$0.2116^{\{1\}}$
		$\hat{\delta}$	$0.1465^{\{6\}}$	$0.1187^{\{4\}}$	$0.1136^{\{2\}}$	$0.1177^{\{3\}}$	$0.1471^{\{7\}}$	$0.3429^{\{8\}}$	$0.1218^{\{5\}}$	$0.0947^{\{1\}}$
		$\hat{\lambda}$	$0.3486^{\{8\}}$	$0.1191^{\{2\}}$	$0.1281^{\{5\}}$	$0.1247^{\{3\}}$	$0.3020^{\{7\}}$	$0.2348^{\{6\}}$	$0.1265^{\{4\}}$	$0.1130^{\{1\}}$
	MRE	$\hat{\alpha}$	$0.2609^{\{6\}}$	$0.2577^{\{4\}}$	$0.2558^{\{3\}}$	$0.2490^{\{1\}}$	$0.3008^{\{7\}}$	$0.4754^{\{8\}}$	$0.2601^{\{5\}}$	$0.2506^{\{2\}}$
		$\hat{\beta}$	$0.2172^{\{8\}}$	$0.2081^{\{6\}}$	$0.2056^{\{4\}}$	$0.2043^{\{3\}}$	$0.2115^{\{7\}}$	$0.1991^{\{2\}}$	$0.2076^{\{5\}}$	$0.1844^{\{1\}}$
		$\hat{\delta}$	$0.0891^{\{6\}}$	$0.0801^{\{4\}}$	$0.0783^{\{2\}}$	$0.0803^{\{5\}}$	$0.0932^{\{7\}}$	$0.1267^{\{8\}}$	$0.0797^{\{3\}}$	$0.0729^{\{1\}}$
		$\hat{\lambda}$	$0.2347^{\{8\}}$	$0.1296^{\{2\}}$	$0.1348^{\{5\}}$	$0.1325^{\{3\}}$	$0.2193^{\{7\}}$	$0.1916^{\{6\}}$	$0.1332^{\{4\}}$	$0.1246^{\{1\}}$
		$\sum Ranks$	$82^{\{7\}}$	$49^{\{4\}}$	$42^{\{3\}}$	$34^{\{2\}}$	$84^{\{8\}}$	$72^{\{6\}}$	$54^{\{5\}}$	$15^{\{1\}}$
300	|BIAS|	$\hat{\alpha}$	$0.3777^{\{4\}}$	$0.3720^{\{3\}}$	$0.3788^{\{5\}}$	$0.3668^{\{2\}}$	$0.4413^{\{7\}}$	$0.8415^{\{8\}}$	$0.3848^{\{6\}}$	$0.3595^{\{1\}}$
		$\hat{\beta}$	$0.3146^{\{2\}}$	$0.3267^{\{7\}}$	$0.3213^{\{5\}}$	$0.3284^{\{8\}}$	$0.3161^{\{3\}}$	$0.3164^{\{4\}}$	$0.3218^{\{6\}}$	$0.2797^{\{1\}}$
		$\hat{\delta}$	$0.2189^{\{6\}}$	$0.1943^{\{4\}}$	$0.1899^{\{2\}}$	$0.1962^{\{5\}}$	$0.2249^{\{7\}}$	$0.3452^{\{8\}}$	$0.1931^{\{3\}}$	$0.1854^{\{1\}}$
		$\hat{\lambda}$	$0.3613^{\{8\}}$	$0.2108^{\{2\}}$	$0.2200^{\{5\}}$	$0.2183^{\{4\}}$	$0.3530^{\{7\}}$	$0.3379^{\{6\}}$	$0.2175^{\{3\}}$	$0.1979^{\{1\}}$
	MSE	$\hat{\alpha}$	$0.23017^{\{3\}}$	$0.2411^{\{4\}}$	$0.2437^{\{5\}}$	$0.2286^{\{2\}}$	$0.3244^{\{7\}}$	$1.4024^{\{8\}}$	$0.2519^{\{6\}}$	$0.2145^{\{1\}}$
		$\hat{\beta}$	$0.1583^{\{2\}}$	$0.1685^{\{6.5\}}$	$0.1675^{\{5\}}$	$0.1725^{\{8\}}$	$0.1618^{\{3\}}$	$0.1645^{\{4\}}$	$0.1685^{\{6.5\}}$	$0.1267^{\{1\}}$
		$\hat{\delta}$	$0.1109^{\{7\}}$	$0.0759^{\{4\}}$	$0.0694^{\{2\}}$	$0.0771^{\{5\}}$	$0.0997^{\{6\}}$	$0.2847^{\{8\}}$	$0.0726^{\{3\}}$	$0.0673^{\{1\}}$
		$\hat{\lambda}$	$0.2141^{\{8\}}$	$0.0780^{\{2\}}$	$0.0867^{\{5\}}$	$0.0835^{\{3\}}$	$0.1990^{\{7\}}$	$0.1934^{\{6\}}$	$0.0863^{\{4\}}$	$0.0731^{\{1\}}$
	MRE	$\hat{\alpha}$	$0.1888^{\{4\}}$	$0.1860^{\{3\}}$	$0.1894^{\{5\}}$	$0.1834^{\{2\}}$	$0.2206^{\{7\}}$	$0.4207^{\{8\}}$	$0.1924^{\{6\}}$	$0.1797^{\{1\}}$
		$\hat{\beta}$	$0.1573^{\{2\}}$	$0.1633^{\{7\}}$	$0.1606^{\{5\}}$	$0.1642^{\{8\}}$	$0.1580^{\{3\}}$	$0.1582^{\{4\}}$	$0.1609^{\{6\}}$	$0.1398^{\{1\}}$
		$\hat{\delta}$	$0.0729^{\{6\}}$	$0.0647^{\{4\}}$	$0.0633^{\{2\}}$	$0.0654^{\{5\}}$	$0.0749^{\{7\}}$	$0.1150^{\{8\}}$	$0.0643^{\{3\}}$	$0.0618^{\{1\}}$
		$\hat{\lambda}$	$0.1806^{\{8\}}$	$0.1054^{\{2\}}$	$0.1100^{\{5\}}$	$0.1091^{\{4\}}$	$0.1765^{\{7\}}$	$0.1689^{\{6\}}$	$0.1087^{\{3\}}$	$0.0989^{\{1\}}$
		$\sum Ranks$	$60^{\{6\}}$	$48.5^{\{2\}}$	$51^{\{3\}}$	$56^{\{5\}}$	$71^{\{7\}}$	$78^{\{8\}}$	$55.5^{\{4\}}$	$12^{\{1\}}$
500	|BIAS|	$\hat{\alpha}$	$0.3000^{\{2\}}$	$0.3015^{\{3\}}$	$0.3052^{\{5\}}$	$0.3016^{\{4\}}$	$0.3357^{\{7\}}$	$0.7387^{\{8\}}$	$0.3103^{\{6\}}$	$0.2867^{\{1\}}$
		$\hat{\beta}$	$0.2602^{\{3\}}$	$0.2752^{\{7\}}$	$0.2700^{\{6\}}$	$0.2761^{\{8\}}$	$0.2618^{\{4\}}$	$0.2580^{\{2\}}$	$0.2664^{\{5\}}$	$0.2328^{\{1\}}$
		$\hat{\delta}$	$0.1916^{\{7\}}$	$0.1700^{\{4\}}$	$0.1642^{\{1\}}$	$0.1778^{\{5\}}$	$0.1913^{\{6\}}$	$0.3456^{\{8\}}$	$0.1669^{\{3\}}$	$0.1650^{\{2\}}$
		$\hat{\lambda}$	$0.2970^{\{7\}}$	$0.1907^{\{4\}}$	$0.1938^{\{5\}}$	$0.1904^{\{3\}}$	$0.2969^{\{6\}}$	$0.3175^{\{8\}}$	$0.1851^{\{2\}}$	$0.1672^{\{1\}}$
	MSE	$\hat{\alpha}$	$0.1436^{\{2\}}$	$0.1589^{\{4\}}$	$0.1563^{\{3\}}$	$0.1600^{\{5\}}$	$0.1861^{\{7\}}$	$1.0850^{\{8\}}$	$0.1635^{\{6\}}$	$0.1395^{\{1\}}$
		$\hat{\beta}$	$0.1104^{\{2\}}$	$0.1225^{\{7\}}$	$0.1202^{\{6\}}$	$0.1248^{\{8\}}$	$0.1111^{\{4\}}$	$0.1105^{\{3\}}$	$0.1155^{\{5\}}$	$0.0905^{\{1\}}$
		$\hat{\delta}$	$0.0792^{\{7\}}$	$0.0565^{\{4\}}$	$0.0515^{\{1\}}$	$0.0628^{\{5\}}$	$0.0790^{\{6\}}$	$0.2805^{\{8\}}$	$0.0537^{\{2\}}$	$0.0538^{\{3\}}$
		$\hat{\lambda}$	$0.1473^{\{7\}}$	$0.0639^{\{4\}}$	$0.0666^{\{5\}}$	$0.0626^{\{3\}}$	$0.1445^{\{6\}}$	$0.1805^{\{8\}}$	$0.0597^{\{2\}}$	$0.0514^{\{1\}}$
	MRE	$\hat{\alpha}$	$0.1500^{\{2\}}$	$0.1507^{\{3\}}$	$0.1526^{\{5\}}$	$0.1508^{\{4\}}$	$0.1678^{\{7\}}$	$0.3693^{\{8\}}$	$0.1551^{\{6\}}$	$0.1433^{\{1\}}$
		$\hat{\beta}$	$0.1301^{\{3\}}$	$0.1376^{\{7\}}$	$0.1350^{\{6\}}$	$0.1380^{\{8\}}$	$0.1309^{\{4\}}$	$0.1290^{\{2\}}$	$0.1332^{\{5\}}$	$0.1164^{\{1\}}$
		$\hat{\delta}$	$0.0638^{\{7\}}$	$0.0567^{\{4\}}$	$0.0547^{\{1\}}$	$0.0592^{\{5\}}$	$0.0638^{\{6\}}$	$0.1152^{\{8\}}$	$0.0556^{\{3\}}$	$0.0550^{\{2\}}$
		$\hat{\lambda}$	$0.1485^{\{7\}}$	$0.0953^{\{4\}}$	$0.0969^{\{5\}}$	$0.0952^{\{3\}}$	$0.1484^{\{6\}}$	$0.1587^{\{8\}}$	$0.0925^{\{2\}}$	$0.0836^{\{1\}}$
		$\sum Ranks$	$56^{\{5\}}$	$55^{\{4\}}$	$49^{\{3\}}$	$61^{\{6\}}$	$69^{\{7\}}$	$79^{\{8\}}$	$47^{\{2\}}$	$16^{\{1\}}$

Table 6. Simulation results for $\boldsymbol{\varphi} = (\beta = 2.75,\ \alpha = 4,\ \delta = 1.5,\ \lambda = 3)^{\intercal}$

n	Est.	Est. Par.	MLEs	LSEs	WLSEs	CRVMEs	MPSEs	PCEs	ADEs	RADEs
50	|BIAS|	$\hat{\alpha}$	$1.1987^{\{6\}}$	$0.7658^{\{2\}}$	$0.8571^{\{5\}}$	$0.7224^{\{1\}}$	$1.2320^{\{7\}}$	1.2505	$0.8523^{\{4\}}$	$0.8501^{\{3\}}$
		$\hat{\beta}$	$1.3812^{\{8\}}$	$0.8305^{\{2\}}$	$0.9486^{\{5\}}$	$0.8658^{\{3\}}$	$0.5293^{\{1\}}$	1.1538	$0.9494^{\{6\}}$	$0.8879^{\{4\}}$
		$\hat{\delta}$	$0.4001^{\{7\}}$	$0.2812^{\{1\}}$	$0.3190^{\{5\}}$	$0.2877^{\{3\}}$	$0.3906^{\{6\}}$	0.4534	$0.3037^{\{4\}}$	$0.2873^{\{2\}}$
		$\hat{\lambda}$	$0.7968^{\{8\}}$	$0.5400^{\{3\}}$	$0.5792^{\{5\}}$	$0.5275^{\{1\}}$	$0.7349^{\{7\}}$	0.6184	$0.5599^{\{4\}}$	$0.5289^{\{2\}}$
	MSE	$\hat{\alpha}$	$2.2618^{\{6\}}$	$1.1757^{\{2\}}$	$1.3435^{\{3\}}$	$1.0186^{\{1\}}$	$2.6189^{\{7\}}$	2.6426	$1.3798^{\{5\}}$	$1.3580^{\{4\}}$
		$\hat{\beta}$	$3.3305^{\{8\}}$	$1.0232^{\{1\}}$	$1.3608^{\{4\}}$	$1.1740^{\{2\}}$	$2.1967^{\{7\}}$	1.9373	$1.3835^{\{5\}}$	$1.2141^{\{3\}}$
		$\hat{\delta}$	$0.4755^{\{8\}}$	$0.1714^{\{1\}}$	$0.2420^{\{5\}}$	$0.2002^{\{3\}}$	$0.3688^{\{6\}}$	0.4493	$0.2234^{\{4\}}$	$0.1913^{\{2\}}$
		$\hat{\lambda}$	$1.0367^{\{8\}}$	$0.4967^{\{3\}}$	$0.5722^{\{5\}}$	$0.4609^{\{1\}}$	$0.8735^{\{7\}}$	0.6563	$0.5423^{\{4\}}$	$0.4733^{\{2\}}$
	MRE	$\hat{\alpha}$	$0.2996^{\{6\}}$	$0.1914^{\{2\}}$	$0.2142^{\{5\}}$	$0.1806^{\{1\}}$	$0.3080^{\{7\}}$	0.3126	$0.2130^{\{4\}}$	$0.2125^{\{3\}}$
		$\hat{\beta}$	$0.5022^{\{8\}}$	$0.3020^{\{1\}}$	$0.3449^{\{4\}}$	$0.3148^{\{2\}}$	$0.4206^{\{7\}}$	0.4195	$0.3452^{\{5\}}$	$0.3228^{\{3\}}$
		$\hat{\delta}$	$0.2667^{\{7\}}$	$0.1875^{\{1\}}$	$0.2126^{\{5\}}$	$0.1918^{\{3\}}$	$0.2604^{\{6\}}$	0.3023	$0.2025^{\{4\}}$	$0.1915^{\{2\}}$
		$\hat{\lambda}$	$0.2656^{\{8\}}$	$0.1800^{\{3\}}$	$0.1930^{\{5\}}$	$0.1758^{\{1\}}$	$0.2449^{\{7\}}$	0.2061	$0.1866^{\{4\}}$	$0.1763^{\{2\}}$
		$\sum Ranks$	$88^{\{8\}}$	$22^{\{1.5\}}$	$56^{\{5\}}$	$22^{\{1.5\}}$	$75^{\{6\}}$	84	$53^{\{4\}}$	$32^{\{3\}}$
150	|BIAS|	$\hat{\alpha}$	$0.8299^{\{6\}}$	$0.5419^{\{2\}}$	$0.6087^{\{4\}}$	$0.5396^{\{1\}}$	$0.9086^{\{7\}}$	1.0640	$0.6207^{\{5\}}$	$0.6046^{\{3\}}$
		$\hat{\beta}$	$0.8630^{\{7\}}$	$0.5667^{\{3\}}$	$0.6386^{\{5\}}$	$0.5657^{\{2\}}$	$0.7396^{\{6\}}$	0.9010	$0.6275^{\{4\}}$	$0.5630^{\{1\}}$
		$\hat{\delta}$	$0.2447^{\{7\}}$	$0.1684^{\{2\}}$	$0.1859^{\{5\}}$	$0.1673^{\{1\}}$	$0.2289^{\{6\}}$	0.3604	$0.1766^{\{4\}}$	$0.1738^{\{3\}}$
		$\hat{\lambda}$	$0.6071^{\{8\}}$	$0.4301^{\{2\}}$	$0.4664^{\{5\}}$	$0.4327^{\{3\}}$	$0.5677^{\{7\}}$	0.5123	$0.4536^{\{4\}}$	$0.3984^{\{1\}}$
	MSE	$\hat{\alpha}$	$1.1728^{\{6\}}$	$0.6126^{\{2\}}$	$0.7282^{\{4\}}$	$0.5948^{\{1\}}$	$1.5048^{\{7\}}$	1.9776	$0.7684^{\{5\}}$	$0.7135^{\{3\}}$
		$\hat{\beta}$	$1.5338^{\{8\}}$	$0.5261^{\{2\}}$	$0.6573^{\{5\}}$	$0.5134^{\{1\}}$	$0.9435^{\{6\}}$	1.2560	$0.6351^{\{4\}}$	$0.5351^{\{3\}}$
		$\hat{\delta}$	$0.2422^{\{7\}}$	$0.0675^{\{2\}}$	$0.0848^{\{5\}}$	$0.0613^{\{1\}}$	$0.1393^{\{6\}}$	0.2750	$0.0719^{\{3\}}$	$0.0726^{\{4\}}$
		$\hat{\lambda}$	$0.6175^{\{8\}}$	$0.3219^{\{2\}}$	$0.3711^{\{5\}}$	$0.3229^{\{3\}}$	$0.5357^{\{7\}}$	0.4648	$0.3554^{\{4\}}$	$0.2822^{\{1\}}$
	MRE	$\hat{\alpha}$	$0.2074^{\{6\}}$	$0.1354^{\{2\}}$	$0.1522^{\{4\}}$	$0.1349^{\{1\}}$	$0.2271^{\{7\}}$	0.2660	$0.1551^{\{5\}}$	$0.1511^{\{3\}}$
		$\hat{\beta}$	$0.3138^{\{7\}}$	$0.2060^{\{3\}}$	$0.2322^{\{5\}}$	$0.2057^{\{2\}}$	$0.2689^{\{6\}}$	0.3276	$0.2281^{\{4\}}$	$0.2047^{\{1\}}$
		$\hat{\delta}$	$0.1631^{\{7\}}$	$0.1122^{\{2\}}$	$0.1239^{\{5\}}$	$0.1115^{\{1\}}$	$0.1526^{\{6\}}$	0.2402	$0.1177^{\{4\}}$	$0.1158^{\{3\}}$
		$\hat{\lambda}$	$0.2023^{\{8\}}$	$0.1433^{\{2\}}$	$0.1554^{\{5\}}$	$0.1442^{\{3\}}$	$0.1892^{\{7\}}$	0.1707	$0.1512^{\{4\}}$	$0.1328^{\{1\}}$
		$\sum Ranks$	$85^{\{7\}}$	$26^{\{2\}}$	$57^{\{5\}}$	$20^{\{1\}}$	$78^{\{6\}}$	89	$50^{\{4\}}$	$27^{\{3\}}$
300	|BIAS|	$\hat{\alpha}$	$0.6675^{\{6\}}$	$0.4337^{\{1\}}$	$0.5023^{\{4\}}$	$0.4375^{\{2\}}$	$0.7489^{\{7\}}$	0.9472	$0.5137^{\{5\}}$	$0.4884^{\{3\}}$
		$\hat{\beta}$	$0.5796^{\{7\}}$	$0.4066^{\{2\}}$	$0.4607^{\{5\}}$	$0.4184^{\{3\}}$	$0.5293^{\{6\}}$	0.7429	$0.4488^{\{4\}}$	$0.3958^{\{1\}}$
		$\hat{\delta}$	$0.1768^{\{7\}}$	$0.1257^{\{1\}}$	$0.1429^{\{5\}}$	$0.1290^{\{2\}}$	$0.1696^{\{6\}}$	0.3111	$0.1396^{\{4\}}$	$0.1356^{\{3\}}$
		$\hat{\lambda}$	$0.4586^{\{8\}}$	$0.3452^{\{3\}}$	$0.3634^{\{5\}}$	$0.3431^{\{2\}}$	$0.4446^{\{6\}}$	0.4518	$0.3480^{\{4\}}$	$0.3075^{\{1\}}$
	MSE	$\hat{\alpha}$	$0.7859^{\{6\}}$	$0.3984^{\{1\}}$	$0.5025^{\{4\}}$	$0.4012^{\{2\}}$	$1.0028^{\{7\}}$	1.5912	$0.5438^{\{5\}}$	$0.4810^{\{3\}}$
		$\hat{\beta}$	$0.6951^{\{7\}}$	$0.2771^{\{1\}}$	$0.3651^{\{5\}}$	$0.3045^{\{3\}}$	$0.4772^{\{6\}}$	0.8842	$0.3499^{\{4\}}$	$0.2815^{\{2\}}$
		$\hat{\delta}$	$0.1166^{\{7\}}$	$0.0325^{\{1\}}$	$0.0485^{\{5\}}$	$0.0370^{\{2\}}$	$0.0663^{\{6\}}$	0.2083	$0.0438^{\{4\}}$	$0.0437^{\{3\}}$
		$\hat{\lambda}$	$0.3752^{\{8\}}$	$0.2168^{\{3\}}$	$0.2422^{\{5\}}$	$0.2168^{\{2\}}$	$0.3479^{\{6\}}$	0.3639	$0.2253^{\{4\}}$	$0.1767^{\{1\}}$
	MRE	$\hat{\alpha}$	$0.1668^{\{6\}}$	$0.1084^{\{1\}}$	$0.1255^{\{4\}}$	$0.1093^{\{2\}}$	$0.1872^{\{7\}}$	0.2368	$0.1284^{\{5\}}$	$0.1221^{\{3\}}$
		$\hat{\beta}$	$0.2107^{\{7\}}$	$0.1478^{\{2\}}$	$0.1675^{\{5\}}$	$0.1521^{\{3\}}$	$0.1925^{\{6\}}$	0.2701	$0.1632^{\{4\}}$	$0.1439^{\{1\}}$
		$\hat{\delta}$	$0.1179^{\{7\}}$	$0.0838^{\{1\}}$	$0.0953^{\{5\}}$	$0.0860^{\{2\}}$	$0.1131^{\{6\}}$	0.2074	$0.0930^{\{4\}}$	$0.0904^{\{3\}}$
		$\hat{\lambda}$	$0.1528^{\{8\}}$	$0.1150^{\{3\}}$	$0.1211^{\{5\}}$	$0.1143^{\{2\}}$	$0.1482^{\{6\}}$	0.1506	$0.1160^{\{4\}}$	$0.1025^{\{1\}}$
		$\sum Ranks$	$84^{\{7\}}$	$20^{\{1\}}$	$57^{\{5\}}$	$27^{\{3\}}$	$75^{\{6\}}$	93	$51^{\{4\}}$	$25^{\{2\}}$
500	|BIAS|	$\hat{\alpha}$	$0.5556^{\{6\}}$	$0.3789^{\{2\}}$	$0.4422^{\{4\}}$	$0.3771^{\{1\}}$	$0.6300^{\{7\}}$	0.8583	$0.4450^{\{5\}}$	$0.4135^{\{3\}}$
		$\hat{\beta}$	$0.4365^{\{7\}}$	$0.3207^{\{2\}}$	$0.3733^{\{5\}}$	$0.3303^{\{3\}}$	$0.4066^{\{6\}}$	0.6092	$0.3639^{\{4\}}$	$0.3003^{\{1\}}$
		$\hat{\delta}$	$0.1487^{\{7\}}$	$0.1106^{\{1\}}$	$0.1241^{\{5\}}$	$0.1123^{\{2\}}$	$0.1418^{\{6\}}$	0.2627	$0.1190^{\{3\}}$	$0.1200^{\{4\}}$
		$\hat{\lambda}$	$0.3646^{\{7\}}$	$0.2877^{\{3\}}$	$0.2986^{\{5\}}$	$0.2856^{\{2\}}$	$0.3609^{\{6\}}$	0.4188	$0.2921^{\{4\}}$	$0.2474^{\{1\}}$
	MSE	$\hat{\alpha}$	$0.5439^{\{6\}}$	$0.3144^{\{2\}}$	$0.3852^{\{4\}}$	$0.3001^{\{1\}}$	$0.7109^{\{7\}}$	1.3160	$0.4008^{\{5\}}$	$0.3472^{\{3\}}$
		$\hat{\beta}$	$0.3559^{\{7\}}$	$0.1860^{\{2\}}$	$0.2528^{\{5\}}$	$0.1970^{\{3\}}$	$0.2880^{\{6\}}$	0.5989	$0.2329^{\{4\}}$	$0.1690^{\{1\}}$
		$\hat{\delta}$	$0.0562^{\{7\}}$	$0.0260^{\{2\}}$	$0.0383^{\{5\}}$	$0.0259^{\{1\}}$	$0.0478^{\{6\}}$	0.1477	$0.0315^{\{4\}}$	$0.0314^{\{3\}}$
		$\hat{\lambda}$	$0.2461^{\{7\}}$	$0.1626^{\{3\}}$	$0.1710^{\{5\}}$	$0.1556^{\{2\}}$	$0.2350^{\{6\}}$	0.3126	$0.1659^{\{4\}}$	$0.1240^{\{1\}}$
	MRE	$\hat{\alpha}$	$0.1389^{\{6\}}$	$0.0947^{\{2\}}$	$0.1105^{\{4\}}$	$0.0943^{\{1\}}$	$0.1575^{\{7\}}$	0.2146	$0.1113^{\{5\}}$	$0.1034^{\{3\}}$
		$\hat{\beta}$	$0.1587^{\{7\}}$	$0.1167^{\{2\}}$	$0.1358^{\{5\}}$	$0.1201^{\{3\}}$	$0.1479^{\{6\}}$	0.2215	$0.1323^{\{4\}}$	$0.1092^{\{1\}}$
		$\hat{\delta}$	$0.0991^{\{7\}}$	$0.0737^{\{1\}}$	$0.0827^{\{5\}}$	$0.0749^{\{2\}}$	$0.0945^{\{6\}}$	0.1751	$0.0793^{\{3\}}$	$0.0800^{\{4\}}$
		$\hat{\lambda}$	$0.1215^{\{7\}}$	$0.0959^{\{3\}}$	$0.0995^{\{5\}}$	$0.0952^{\{2\}}$	$0.1203^{\{6\}}$	0.1396	$0.0973^{\{4\}}$	$0.0825^{\{1\}}$
		$\sum Ranks$	$81^{\{7\}}$	$25^{\{2\}}$	$57^{\{5\}}$	$23^{\{1\}}$	$75^{\{6\}}$	96	$49^{\{4\}}$	$26^{\{3\}}$

Table 7. Partial and overall ranks of all methods of estimation for several parametric values

$\boldsymbol{\varphi}^{\top}$	n	MLE	OLSE	WLSE	CRVME	MPSE	PCE	ADE	RADE
$(\hat{\beta}=0.75,\ \hat{\alpha}=0.5,\ \hat{\delta}=1.25,\ \hat{\lambda}=0.25)$	50	8	4.5	6	3	7	1	4.5	2
	150	7.5	4.5	6	4.5	7.5	1	3	2
	300	7.5	3.5	6	5	7.5	2	3.5	1
	500	7	3	6	5	8	2	4	1
$(\hat{\beta}=0.5,\ \hat{\alpha}=0.5,\ \hat{\delta}=1.25,\ \hat{\lambda}=0.5)$	50	7.5	4	6	3	7.5	1	5	2
	150	7.5	4	5	3	7.5	1	6	2
	300	7.5	2.5	5	2.5	7.5	1	6	4
	500	7.5	3	5	1.5	7.5	1.5	6	4
$(\hat{\beta}=2,\ \hat{\alpha}=0.75,\ \hat{\delta}=1.5,\ \hat{\lambda}=2.5)$	50	7	3	5	2	6	8	4	1
	150	7	5	2	3	6	8	4	1
	300	6	4	2	5	7	8	3	1
	500	6.5	4	3	5	6.5	8	1.5	1.5
$(\hat{\beta}=2.00,\ \hat{\alpha}=2.00,\ \hat{\delta}=3.00,\ \hat{\lambda}=2.00)$	50	8	3	5	2	7	6	4	1
	150	7	4	3	2	8	6	5	1
	300	6	2	3	5	7	8	4	1
	500	5	4	3	6	7	8	2	1
$(\hat{\beta}=2.75,\ \hat{\alpha}=4.00,\ \hat{\delta}=1.5,\ \hat{\lambda}=3.00)$	50	8	1.5	5	1.5	6	7	4	3
	150	7	2	5	1	6	8	4	3
	300	7	1	5	3	6	8	4	2
	500	7	2	5	1	6	8	4	3
$(\hat{\beta}=0.5,\ \hat{\alpha}=5.00,\ \hat{\delta}=4.00,\ \hat{\lambda}=0.25)$	50	8	1	4	3	7	2	5	6
	150	7	1	3	2	8	4	5	6
	300	7	1	3	2	8	5	4	6
	500	7	1	2	3	8	5	4	6
$(\hat{\beta}=0.5,\ \hat{\alpha}=0.5,\ \hat{\delta}=6.00,\ \hat{\lambda}=7.00)$	50	6.5	4	5	3	6.5	8	2	1
	150	7	4	5	3	6	8	2	1
	300	7	4	5	3	6	8	2	1
	500	7	4	3	5	6	8	1	2
$(\hat{\beta}=2.00,\ \hat{\alpha}=1.00,\ \hat{\delta}=1.5,\ \hat{\lambda}=2.5)$	50	7	4	1	3	6	8	5	2
	150	6	5	1	4	7	8	3	2
	300	6	5	1	3	7	8	4	2
	500	5	4	1	7	6	8	3	2
$\sum$*Ranks*		222	102.5	125	105	220	181.5	121.5	74.5
Overall Rank		8	2	5	3	7	6	4	1

6. Real-data applications

Three real-world data applications are given in this part to demonstrate the versatility and usefulness of the NEHTLx distribution. According to Lee and Wang [25], the first data set shows the remission times (in months) of patients with bladder cancer that cost 128.

The US government's Federal Trade Commission gathered data on nicotine readings from various brands of cigarettes in 1998 for the second data set. This paper, Tar, Nicotine, and Carbon Monoxide from 346 Different Domestic Cigarette Varieties, was published in 1998. The two datasets are given in Appendix A. Table 8 showed ML estimates (first line) and SEs (second line) for the first data and Table 9 showed ML estimates (first line) and SEs (second line) for the second data.

Table 8. The ML estimates (first line) and SEs (second line) for the first data

NEHTLx (β, α, δ, λ)	0.2266	0.2362		20.6907	16.6029
	0.0764	0.0269		0.4810	0.3695
KwLx (β, α, a, b)	0.1345		10.3074	1.5148	46.2536
	3.0118		28.2922	0.2708	1,382.0882
OEHLLx (β, α, a, b)	1.4352	25.6174		0.1079	9.5646
	0.3414	392.8704		1.3575	30.3475
EOWLx (β, α, a, b)	1.3878	1.1017		3.3523	26.7780
	0.1869	1.0348		6.2823	49.8604
BELx (β, δ, λ, a, b)	1.9626	3.0891	0.0473	0.7897	1.4012
	4.3429	6.3440	0.0559	1.8160	2.3892
FTLLx (β, δ, λ, a, b)	0.3349	78.0702	0.5045	4.4559	8.8993
	0.1579	98.5832	0.7081	2.2444	3.2043
PLx (β, λ, γ)			2.3348	1	0.2337
			0.4435	0.3059	0.0572
Lx (a, b)				13.9384	121.0225
				15.3849	142.7058

Table 9. The ML estimates (first line) and SEs (second line) for the second data

NEHTLx (β, α, δ, λ)	0.0052	2.1436		1.5425	9.8283
	0.0010	0.6008		0.5245	2.5685
KwLx (β, α, a, b)	303.4025		7,264.3204	2.7686	7,928.7791
	113.6507		106.6897	0.1206	7,436.3940
OEHLLx (β, α, a, b)	1.8469	0.6890		8.6928	5.5263
	0.2689	0.2880		7.5845	5.8120
EOWLx (β, α, a, b)	2.2563	0.2194		476.1364	633.6349
	0.1472	0.0988		261.4638	347.6861
BELx (β, δ, λ, a, b)	5.5032	9.7581	0.0561	0.5090	64.5054
	1.9867	6.0557	0.0365		
FTLLx (β, δ, λ, a, b)	0.2413	7,795.4775	0.7728	1,401.4123	219.8809
	0.0094	4,000.2086	0.4025	0.5550	0.5825
PLx (β, λ, γ)			3	1	1.8157
			0.1459	0.1666	0.2300
Lx (a, b)				12,555.750	10,704.890
				705.0574	177.8126

The fitting performance of the NEHTLx distribution is contrasted with those of a few competing Lx distributions, namely the power-Lx (PLx) [15], extended odd Weibull Lx (EOWL)[12], odd exponentiated half-logistic Lx (OEHLLx) [11], beta exponentiated Lx (BEL) [13], Fréchet Topp-Leone Lx (FTLLx) [14], power-Lx (PLx) [15], and Lx distributions.

The information criteria (IC) used to compare the fitted distributions are the following: the KS p-value, the Cramér-Von Mises (W^*), the Anderson-Darling (A^*), the Bayesian IC (BIC), the Hannan-Quinn IC (HQIC), and the Akaike IC (AIC), consistent AIC (CAIC), and some goodness-of-fit statistics. The numerical results in this section are obtained using the R software.

The ML estimates and standard errors (SEs) of the fitted models for the two analysed data sets are presented in Tables 8 and 9, respectively. Tables 10 and 11 list the values of AIC, CAIC, BIC, HQIC, W^*, A^*, KS, and p-value for the NEHTLx distribution and the KwLx, OEHLLx, EOWLx, BELx, FTLLx, PLx, and Lx distributions. Among all fitted models, it is observed that the NEHTLx distribution has the biggest p-value and the lowest goodness-of-fit statistics. Therefore, for both data sets, the two applications demonstrate how well the NEHTLx distribution fits.

In addition, Figures 5 and 6, which display the fitted density, CDF, SF, and (probability-probability) P-P plots of the NEHTLx distribution, provide a visual exploration of the distribution's superior fit for both data sets. Furthermore, for both data sets, the P-P plots of all competing models are shown in Figures 7 and 8. The results in Tables 10 and 11 are corroborated by these plots.

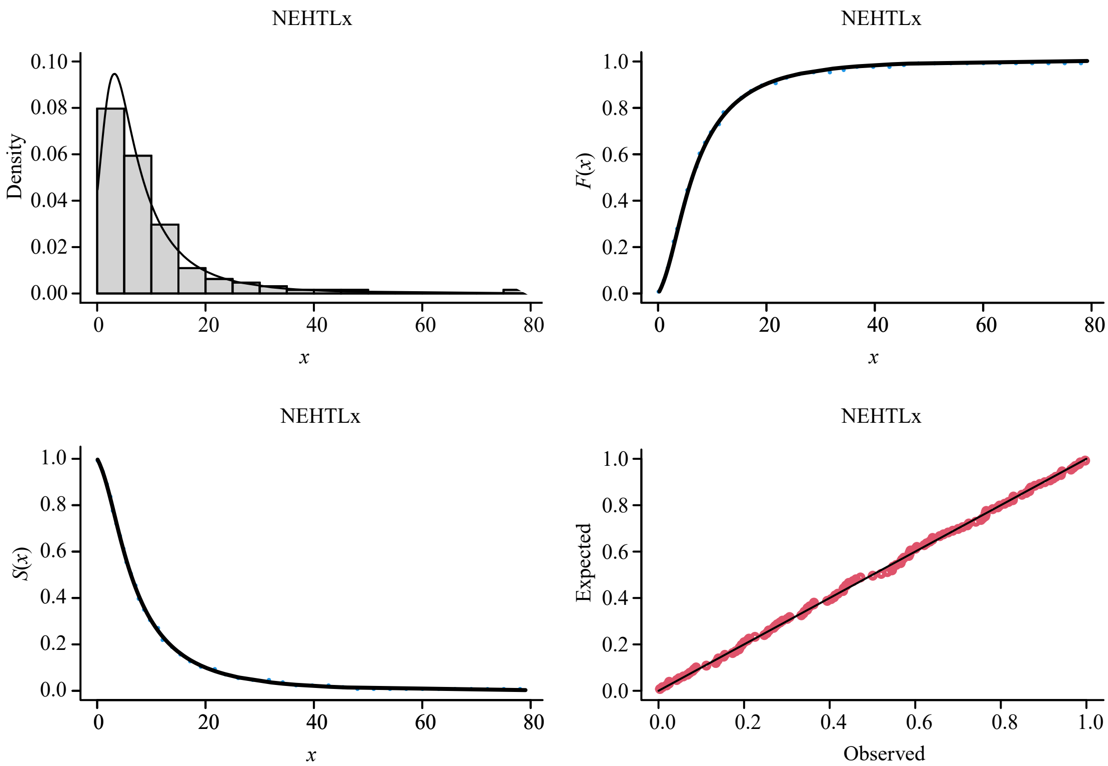

Figure 5. Plots of the fitted functions of the NEHTLx distribution for first data

Table 10. The findings of the first data for all compared distributions

Model	AIC	CAIC	BIC	HQIC	W^*	A^*	KS	p-value
NEHTLx	826.4548	826.7800	837.8630	831.0900	0.0119	0.0746	0.0300	0.9998
KwLx	827.9002	828.2254	839.3084	832.5354	0.0263	0.1757	0.0392	0.9892
OEHLLx	827.4570	827.7822	838.8651	832.0921	0.0210	0.1396	0.0363	0.9957
EOWLx	827.2225	827.5477	838.6307	831.8577	0.0181	0.1223	0.0331	0.9989
BELx	830.0076	830.4994	844.2678	835.8016	0.0270	0.1808	0.0399	0.9866
FTLLx	828.8664	829.3582	843.1266	834.6604	0.0162	0.1022	0.0339	0.9984
PLx	913.0332	913.2267	921.5893	916.5096	0.7497	4.5549	0.2506	0
Lx	831.6658	831.7618	837.9698	833.9834	0.0806	0.4873	0.0966	0.1826

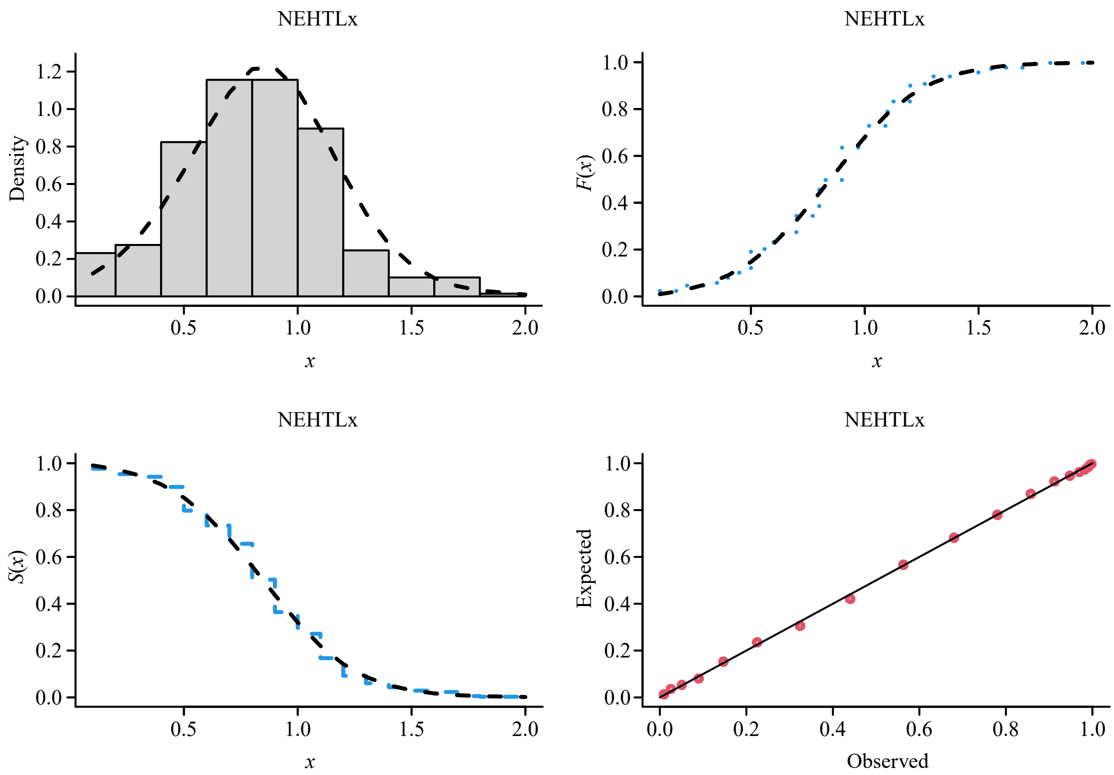

Figure 6. Plots of the fitted functions of the NEHTLx distribution for second data

Table 11. The findings of the second data for all compared distributions

Model	AIC	CAIC	BIC	HQIC	W^*	A^*	KS	p-value
NEHTLx	222.9341	223.0514	238.3199	229.0608	0.3415	1.8679	0.0962	0.0033
KwLx	235.9617	236.0790	251.3475	242.0884	0.5181	3.0125	0.1181	0.0001
OEHLLx	228.4994	228.6167	243.8852	234.6261	0.4053	2.3334	0.1044	0.0010
EOWLx	229.6229	229.7402	245.0087	235.7496	0.4338	2.4849	0.1091	0.0005
BELx	236.9882	237.1647	256.2204	244.6465	0.4930	2.8945	0.1163	0.0001
FTLLx	274.1717	274.3482	293.4039	281.8300	1.0247	5.9073	0.1524	0
PLx	271.5294	271.5996	283.0687	276.1244	0.9995	5.8101	0.1840	0
Lx	585.6746	585.7096	593.3675	588.7380	1.1062	6.5418	0.3425	0

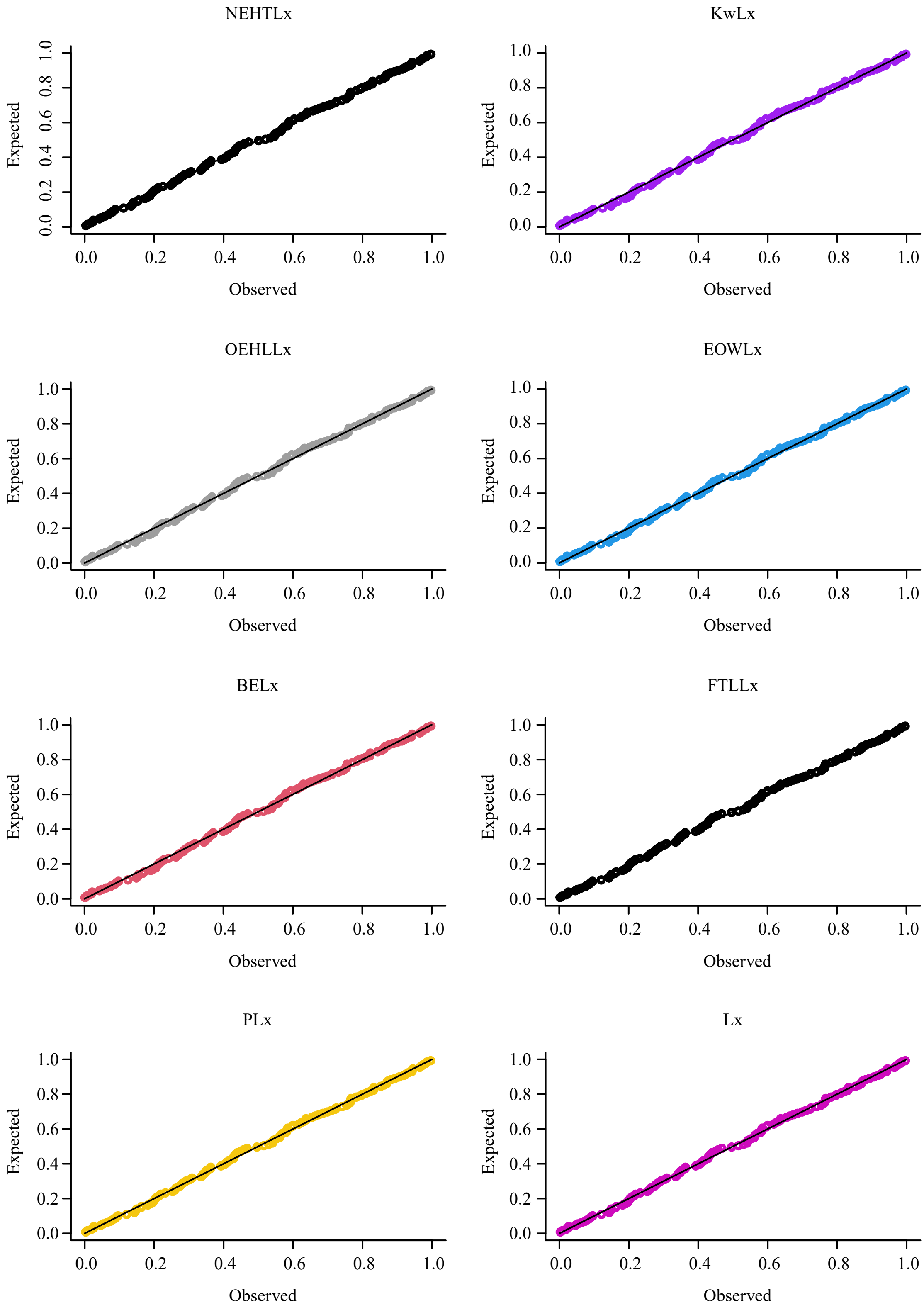

Figure 7. P-P plots of the NEHTLx distribution with other distributions for first data

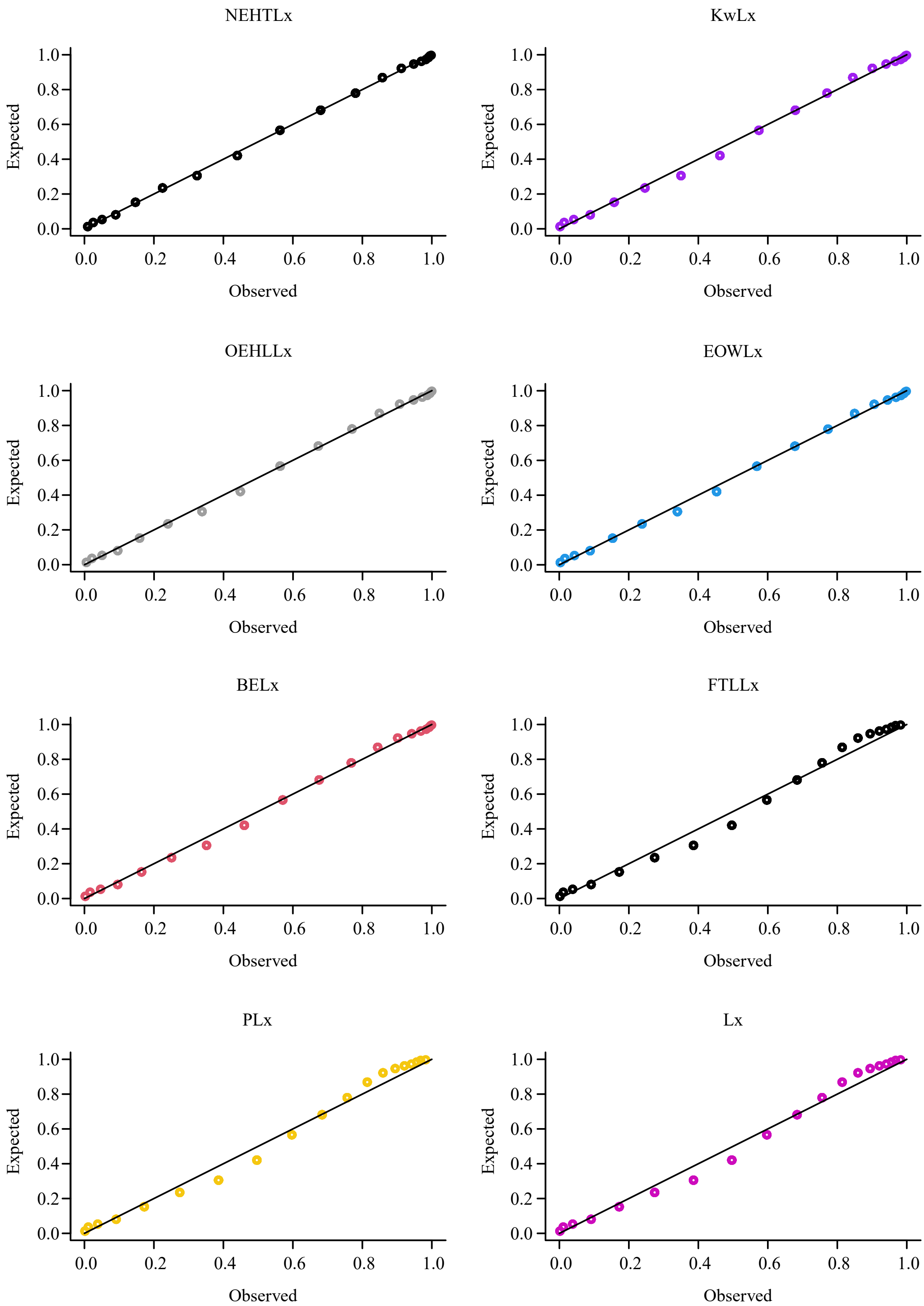

Figure 8. P-P plots of the NEHTLx distribution with other distributions for second data

7. Concluding remarks

The new extended heavy-tailed Lomax (NEHTLx) distribution was presented in this study as a flexible extension of the Lomax model. The NEHTLx density can be represented as a combination of Lomax densities. Its failure rate shows bathtub, reversed J, unimodal, and decreasing shapes. The NEHTLx model's mathematical properties are determined. Moreover, several traditional estimation methods are used to estimate the NEHTLx parameters. Extensive simulations are presented to explore the performance and accuracy of the estimation approaches. The numerical results showed that the right-tail Anderson-Darling and least squares methods outperform all other estimation methods with overall scores of 74.5 and 102.5, respectively. Hence, based on the conducted simulations, those two methods can be recommended for estimating the NEHTLx parameters. Finally, the practical importance and flexibility of the NEHTLx distribution are addressed by two applications to real-life data. Goodness-of-fit metrics showed that the NEHTLx distribution provides a better fit in comparison with other Lomax distributions.

Acknowledgement

The author extends his appreciation to Taif University, Saudi Arabia, for supporting this work through project number (TU-DSPP-2024-162).

Data availability

This work is mainly a methodological development, which has been applied to secondary data as stated in the manuscript.

Conflicts of interest

The author declares no conflicts of interest.

References

[1] Lomax KS. Business failures: Another example of the analysis of failure data. *Journal of the American Statistical Association*. 1954; 49(268): 847-852.

[2] Chahkandi M, Ganjali M. On some lifetime distributions with decreasing failure rate. *Computational Statistics & Data Analysis*. 2009; 53(12): 4433-4440.

[3] Balkema AA, De Haan L. Residual life time at great age. *The Annals of Probability*. 1974; 2(5): 792-804.

[4] Johnson NL, Kotz S. *Continuous Multivariate Distributions*. New York: Wiley; 1972.

[5] Arnold BC. Pareto and generalized Pareto distributions. In: Chotikapanich D. (ed.) *Modeling Income Distributions and Lorenz Curves*. 2nd ed. New York: Springer; 2008. p.119-145.

[6] Ghitany ME, Al-Awadhi FA, Alkhalfan L. Marshall-Olkin extended Lomax distribution and its application to censored data. *Communications in Statistics-Theory and Methods*. 2007; 36(10): 1855-1866.

[7] Abdul-Moniem IB, Abdel-Hameed HF. On exponentiated Lomax distribution. *International Journal of Mathematical Archive*. 2012; 3: 2144-2150.

[8] Lemonte AJ, Cordeiro GM. An extended Lomax distribution. *Statistics*. 2011; 47(4): 800-816.

[9] Cordeiro GM, Ortega EMM, Popović BV. The gamma-Lomax distribution. *Journal of Statistical Computation and Simulation*. 2015; 85(2): 305-319.

[10] Tahir MH, Cordeiro GM, Mansoor M, Zubair M. The Weibull-Lomax distribution: Properties and applications. *Hacettepe Journal of Mathematics and Statistics*. 2015; 44(2): 455-474.

[11] Afify AZ, Altun E, Alizadeh M, Ozel G, Hamedani GG. The odd exponentiated half-logistic-G family: Properties, characterizations and applications. *Chilean Journal of Statistics*. 2017; 8(2): 65-91.

[12] Alsuhabi H, Alkhairy I, Almetwally EM, Almongy HM, Gemeay AM, Hafez EH, et al. A superior extension for the Lomax distribution with application to COVID-19 infections real data. *Alexandria Engineering Journal*. 2022; 61(12): 11077-11090.

[13] Mead ME. On five-parameter Lomax distribution: Properties and applications. *Pakistan Journal of Statistics and Operation Research*. 2016; 12(1): 185-199.

[14] Reyad H, Korkmaz MC, Afify AZ, Hamedani GG, Othman S. The Fréchet Topp Leone-G family of distributions: Properties, characterizations and applications. *Annals of Data Science*. 2021; 8: 345-366.

[15] Rady EA, Hassanein WA, Elhaddad TA. The power Lomax distribution with an application to bladder cancer data. *SpringerPlus*. 2016; 5: 1-22.

[16] Qura ME, Alqawba M, Al Sobhi MM, Afify AZ. A novel extended Power-Lomax distribution for modeling real-life data: Properties and inference. *Journal of Mathematics*. 2023; 2023(1): 6661792.

[17] Al Abbasi JN, Afify AZ, Alnssyan B, Shama MS. The Lambert-G family: Properties, inference, and applications. *CMES-Computer Modeling in Engineering & Sciences*. 2024; 140(1): 513-536.

[18] Jamal F, Alqawba M, Altayab Y, Iqbal T, Afify AZ. A unified exponential-H family for modeling real-life data: Properties and inference. *Heliyon*. 2024; 10(6): e27661.

[19] Aljohani HM, Bandar SA, Al-Mofleh H, Ahmad Z, El-Morshedy M, Afify AZ. A new asymmetric extended family: Properties and estimation methods with actuarial applications. *PLOS ONE*. 2022; 17: e0275001.

[20] Moors JJA. A quantile alternative for kurtosis. *Journal of the Royal Statistical Society: Series D (The Statistician)*. 1988; 37(1): 25-32.

[21] Galton F. *Inquiries Into Human Faculty and Its Development*. London: Macmillan; 1883.

[22] Aloafi TA, Aljohani HM. An overview of composite standard Elastic-Net distribution based on complex wavelet coefficients. *Journal of Mathematics*. 2022; 2022(1): 9005413.

[23] Kao JHK. Computer methods for estimating Weibull parameters in reliability studies. *IRE Transactions on Reliability and Quality Control*. 1958; PGRQC-13: 15-22.

[24] Kao JHK. A graphical estimation of mixed Weibull parameters in life-testing of electron tubes. *Technometrics*. 1959; 1(4): 389-407.

[25] Lee ET, Wang J. *Statistical Methods for Survival Data Analysis*. New York: John Wiley & Sons; 2003.

Appendix A

Bladder cancer dataset

2.46, 3.64, 5.09, 7.26, 9.47, 14.24, 25.82, 0.51, 2.54, 3.70, 5.17, 7.28, 3.88, 5.32, 7.39, 10.34, 14.83, 34.26, 0.90, 2.69, 4.18, 5.34, 7.59, 10.66, 11.79, 18.10, 1.46, 4.40, 5.85, 8.26, 11.98, 19.13, 1.76, 3.25, 4.50, 6.25, 12.07, 21.73, 2.07, 3.36, 6.93, 8.65, 12.63, 22.69, 4.26, 5.41, 7.63, 17.12, 46.12, 1.26, 2.83, 4.33, 5.49, 7.66, 11.25, 17.14, 0.08, 2.09, 3.48, 4.87, 6.94, 8.66, 13.11, 23.63, 0.20, 2.23, 3.52, 4.98, 9.74, 14.76, 26.31, 0.81, 2.62, 3.82, 5.32, 7.32, 10.06, 14.77, 32.15, 2.64, 8.37, 12.02, 2.02, 3.31, 4.51, 6.54, 8.53, 12.03, 20.28, 2.02, 3.36, 6.76, 15.96, 36.66, 1.05, 2.69, 4.23, 5.41, 7.62, 10.75, 16.62, 43.01, 1.19, 2.75, 79.05, 1.35, 2.87, 5.62, 7.87, 11.64, 17.36, 1.40, 3.02, 4.34, 5.71, 7.93, 6.97, 9.02, 13.29, 0.40, 2.26, 3.57, 5.06, 7.09, 9.22, 13.80, 25.74, 0.50.

Nicotine datasets

1.1, 0.2, 0.8, 0.5, 1.1, 0.1, 0.8, 1.7, 1.0, 0.8, 1.0, 0.8, 1.0, 0.2, 0.8, 0.4, 1.0, 0.2, 0.8, 1.4, 0.8, 0.5, 1.1, 0.9, 1.3, 0.9, 0.4, 1.7, 1.4, 1.0, 0.7, 0.4, 0.9, 0.7, 0.8, 0.7, 0.4, 0.9, 0.6, 0.4, 1.2, 2.0, 0.7, 0.5, 0.9, 0.5, 0.9, 0.7, 0.9, 0.7, 0.4, 1.0, 0.7, 0.9, 1.3, 1.0, 1.2, 0.9, 1.1, 0.8, 0.5, 1.0, 0.7, 0.5, 1.7, 1.1, 0.8, 0.5, 1.2, 0.8, 1.1, 0.9, 1.2, 0.9, 0.8, 0.6, 0.3, 0.8, 0.6, 0.4, 1.1, 1.0, 1.1, 1.1, 0.9, 1.1, 0.8, 1.0, 0.7, 1.6, 0.8, 0.6, 0.8, 0.6, 1.2, 0.9, 0.6, 0.8, 1.0, 0.5, 0.8, 1.0, 1.1, 0.8, 0.8, 0.5, 1.1, 0.8, 1.4, 0.9, 0.5, 1.7, 0.9, 0.8, 0.8, 1.2, 0.9, 0.8, 0.5, 1.0, 0.6, 0.1, 0.2, 0.5, 0.1, 0.1, 0.9, 0.6, 0.9, 0.6, 1.2, 1.5, 1.1, 1.4, 1.2, 0.8, 0.8, 0.6, 0.4, 1.2, 1.3, 1.0, 0.6, 1.2, 0.9, 1.2, 0.9, 0.5, 0.8, 1.0, 0.7, 0.9, 1.0, 0.1, 0.2, 0.1, 0.1, 1.1, 1.0, 1.1, 0.7, 1.1, 1.5, 1.5, 1.0, 0.8, 1.0, 0.5, 1.7, 0.3, 0.6, 0.6, 0.4, 0.5, 0.5, 0.7, 0.4, 0.5, 0.8, 0.5, 1.3, 0.9, 1.3, 0.9, 0.5, 1.2, 0.9, 1.1, 0.9, 0.5, 0.7, 0.5, 1.1, 1.1, 0.5, 0.8, 0.6, 1.2, 0.8, 0.4, 1.3, 0.8, 0.5, 1.2, 0.7, 0.5, 0.9, 1.3, 0.8, 1.2, 0.9, 1.1, 0.8, 0.6, 1.1, 0.8, 1.1, 0.8, 1.5, 1.1, 0.8, 0.4, 1.0, 0.8, 1.4, 0.9, 0.9, 1.0, 0.9, 1.3, 0.8, 1.0, 0.5, 1.0, 0.7, 0.5, 1.4, 1.2, 0.7, 0.5, 1.3, 0.9, 0.8, 1.0, 0.7, 0.7, 0.6, 0.8, 1.1, 0.9, 0.9, 0.8, 0.8, 0.7, 0.7, 0.4, 0.5, 0.4, 0.9, 0.9, 0.7, 1.0, 1.0, 0.7, 1.3, 0.9, 1.1, 0.8, 1.2, 1.1, 1.2, 1.1, 1.2, 0.2, 0.5, 0.7, 0.2, 0.5, 0.6, 0.1, 0.4, 0.6, 0.2, 0.5, 1.1, 0.8, 0.6, 1.1, 0.9, 0.6, 0.3, 0.9, 0.7, 1.8, 1.2, 0.9, 1.7, 1.2, 1.3, 1.2, 0.9, 0.7, 0.7, 1.2, 1.0, 0.9, 1.6, 0.8, 0.8, 1.1, 1.1, 0.8, 0.6, 1.0, 0.8, 1.1, 0.8, 0.5, 1.5, 0.9, 1.1, 0.9, 1.1, 1.0, 0.9, 1.2, 0.9, 1.2, 0.9, 0.5, 0.9, 0.7, 0.3, 1.0, 0.6, 1.0, 0.9, 1.0, 1.1, 0.8, 0.5, 1.1, 0.8, 1.2, 0.8, 0.5.